Equation of State and Transport Coefficients of Quark-Gluon Plasma using Cluster Expansion Method

Thesis submitted to the University of Calicut
in partial fulfillment of the requirements
for the the degree of

Doctor of Philosophy
in
Physics
Under the Faculty of Science

Prasanth J. P.

Department of Physics
University of Calicut
Malappuram
Kerala - 673635.

October 2018

CERTIFICATE

Certified that the work presented in this thesis entitled 'Equation of State and Transport Coefficients of Quark-Gluon Plasma using Cluster Expansion Method' is a bonafide work done by Mr. Prasanth J. P., under my guidance in the Department of Physics, University of Calicut and this work has not been included in any other thesis submitted previously for the award of any degree.

University of Calicut
October 2018

Dr. Vishnu Mayya Bannur
(Supervising Guide)

CERTIFICATE

This is to certify that the thesis titled 'Equation of State and Transport Coefficients of Quark-Gluon Plasma using Cluster Expansion Method' has been checked for plagiarism, using the URKUND software, at the CHMK library, University of Calicut. Also, no changes were suggested by the thesis referees after evaluation, and therefore, there are no further corrections to be made in this thesis. The contents in the hard copy and soft copy of the thesis are same.

University of Calicut

Dr. Vishnu Mayya Bannur

DECLARATION

I hereby declare that the work presented in this thesis entitled 'Equation of State and Transport Coefficients of Quark-Gluon Plasma using Cluster Expansion Method' is based on the original work done by me under the guidance of Dr.Vishnu Mayya Bannur, Department of Physics, University of Calicut, and has not been included in any other thesis submitted previously for the award of any degree.

University of Calicut
October 2018 Prasanth J. P.

Acknowledgements

I express my sincere gratitude to Dr. Vishnu Mayya Bannur, for suggesting the problem, for his guidance and for providing the freedom to pursue the problem in my own way. I thank Dr. K. M. Udayanandan, Nehru Arts and Science College, Kanhangad, for giving me an initial thrust to the field of Quark-Gluon Plasma. I am grateful to him for his kind discussions. I owe greatly to Prof. Bijan Sheikh-Sabzevari, Italian National Research Council, for giving necessary feedback and providing reference articles in the area of Cluster expansion method. I express my heartfelt thanks to Dr. P.P. Pradyumnan, HoD, for the support during the course of this work.

I thank my co-researchers, Sebastian Koothottil, Shyam Kumar A.M., Simji. P, Sreejith Sivaraman, Sineeba Ramadas, friends, teachers and non-teaching staff at the Department of Physics, University of Calicut, for their constant encouragement and support. I am greatly indebted to Kerala Shasthra Sahithya Parishath for kindling my interest in science research through their efforts to build a scientific tempered society. I express my deep gratitude and love to my life partner Subina S., for her immense encouragements.

I thank University Grants Commission, New Delhi, for granting fellowship to carry out this research work.

Prasanth J. P.

All life is problem solving

-Karl Popper-

Contents

List of Figures

List of Tables

List of papers published/communicated:

1. Transport coefficients of Quark–Gluon plasma with full QCD potential, **Prasanth. J. P** and Vishnu Mayya Bannur, *Physica A 498, 10–16 (2018).*

2. Quark-gluon plasma phase transition using cluster expansion method, Syamkumar A. M., **Prasanth. J. P** and Vishnu Mayya Bannur, *Physica A 432, 71–75 (2015).*

3. Hadron Formation in a Non-Ideal Quark Gluon Plasma Using Mayer's Method of Cluster, **Prasanth. J. P** and Vishnu Mayya Bannur, *Proc. Indian Natn Sci Acad 81, 158-164 (2015).*

4. Revisiting Cornell potential model of the Quark-Gluon plasma, **Prasanth. J. P**, Sebastian Koothottil and Vishnu Mayya Bannur, *Physica A (Under Review)(2018).*

5. Thermodynamics of non-ideal QGP using Mayers cluster expansion method, **Prasanth. J. P**, Simji. P and Vishnu Mayya Bannur, *Proc of the DAE Symp. on Nucl. Phys. 58, 774-775 (2013).*

6. Gluon plasma thermodynamics: from transition region to SB limit, Simji. P, **Prasanth. J. P** and Vishnu Mayya Bannur, *Proc. of the DAE Symp. on Nucl. Phys. 58, 772-773 (2013).*

7. Equation of state of a strongly coupled Quark Gluon Plasma using Cornell Potential, Sebastian Koothottil, **Prasanth. J. P**, and Vishnu Mayya Bannur, *DAE Symp. Nucl. Phys.61, 814-815 (2016).*

8. Cornell Potential Model for Strongly Coupled Quark Gluon Plasma, Sebastian Koothottil, **Prasanth. J. P** and Vishnu Mayya Bannur, *DAE Symp. Nucl. Phys.62, 912-913 (2017).*

List of Conference/ Seminars/ Symposium attended:

1. Thermodynamics of non-ideal QGP using Mayer's cluster expansion method, International Symposium on Nuclear Physics, *Baba atomic research centre-Mumbai-400085; December 2-6, 2013.*

2. Hadron Formation in a Non-Ideal Quark Gluon Plasma Using Mayers Method of Cluster Expansion, *International conference on matter at extreme condition: Then and Now (ICMEC), Bose Institute-Kolkatha, January 15-17, 2014.*

3. Viscosity Of The QGP Using Screened Cornell Potential, *29th National Symposium on Plasma Science Technology and the International Conference on Plasma Nanotechnology (Plasma-2014), Mahatma Gandhi University, Kottayam, Kerala, December 8-11, 2014.*

4. Quark-Gluon Plasma Phase Transition using cluster expansion method, *7-th International Conference on Physics and Astrophysics of Quark Gluon Plasma (ICPAQGP-2015), VECC, Kolkata, India, February 1-6, 2015.*

5. Shear Viscosity Of The QGP Using Mayers Cluster expansion method, *7-th International Conference on Physics and Astrophysics of Quark Gluon Plasma (ICPAQGP-2015), VECC, Kolkata, India, February 1-6, 2015.*

Preface

The question of the possible states of matter leads us to the world of elementary constituents and their interactions. The strongly interacting quarks and gluons in the limit of high temperatures and/or baryon densities form the quark-gluon plasma. The study of quark-gluon plasma and its thermodynamics is significant in understanding the small and large scale structure of the universe.

This thesis focuses on theoretical tools which can be used in the framework of cluster expansion method to tackle the physics of the quark gluon plasma. We examine the equation of state of quark-gluon plasma, quarkonium dissociation studies, transport coefficients of quark-gluon plasma and the phase transition studies under the background of cluster expansion method.

The structure of the thesis is as follows. First Chapter describes a basic introduction to quark-gluon plasma, signature of quark-gluon plasma, experimental investigations, lattice QCD works and the history of theoretical models on quark-gluon plasma.

In Chapter 2, a study of quarkonium dissociation and multi-strange particle enhancement are carried out on the footing of the Mayer's cluster expansion method, which have been pointed out a possible signature for the occurrence of quark-gluon plasma in relativistic heavy ions collisions. An equation of state is derived, which is applicable for different species of quark system and we investigated the criterion for the temperature, where heavy quarkonium like charmonium ($J/\psi(c,\bar{c})$) and bottomonium ($\Upsilon(b,\bar{b})$) suppression occurs. This equation of state has been studied by using Cornell potential with the effect of screening. We have obtained equation of state in terms of number density and studied multi-strange hadronisation process.

The prime focus of Chapter 3 is the phase transition studies of quark-gluon plasma, using the mathematical formalism of cluster expansion method which is extended by Ushcats in the case of condensation studies. Cluster expansion equation of state for finite size system (fEoS) and equation of state in the thermodynamic limit (CEEoS) for modified Cornell potential are plotted. The critical

point where the system converges has been obtained for different temperatures and number of particles. A comparative study between Mayer's equation of state and Ushcats equation of state has been investigated with modified Cornell potential.

Chapter 4 describes the effects of transport coefficients such as, the ratio of shear viscosity to entropy density and bulk viscosity to entropy density in the relativistic heavy-ion collisions, in particular near the transition region. Mayer's theory of plasma is used to derive a compact expression for the equation of state of quark-gluon plasma. We have used modified Cornell potential to take into account the interaction between partons in the quark-gluon plasma. To calculate the transport coefficients, we have used the Chapman-Enskog method. The Chapman-Enskog approximation relates the transport cross section with the interaction potential.

In Chapter 5, we derived a semi-classical equation of state for quark-gluon plasma, including the quantum aspects in the strongly coupled regime. Here we have used the quantum cluster expansion which takes into account the contribution of binary bound states of quarks and gluons near the critical temperature T_c, we obtain a better fit with lattice QCD results. Here we investigated pressure, energy density and velocity of sound of quark-gluon plasma using the modified equation of state. We extend our work upto 1000 T_c range. Finally a comparative study of our modified equation of state with the earlier study using Mayer's theory of plasma is presented.

Chapter 6 summarizes the findings of the thesis and describes future prospects of this work. The key element of our approach is to develop an exact equation of state and transport coefficients for the quark-gluon plasma in the framework of cluster expansion. The theory of quark-gluon plasma is rapidly developing, both on classical and quantum level and eventually leading to help the complete description of the Universe.

Chapter 1

The Physics of the Quark-Gluon Plasma

1.1 Introduction

The scientific discoveries of the fundamental constituents of matter and their interactions help to frame a language about the early Universe. The study of matter is very important to understand the nature in the smallest and the largest space and time scales. We cannot return space-time to the initial configuration to address the philosophical as well as scientific quest of the early universe, but we can effectively turn back the clock by doing the experiments at high energy scale. The Quark-Gluon Plasma (QGP) is a primordial form of quantum chromodynamics (QCD) matter at high temperature and/or baryon number density. The characteristic values at which the transition from hadrons to QGP happens correspond to $T_c \approx 10^{12}K$ and $\rho_c \approx 10^{15}g/cm^3$. Study of QGP in the laboratory provides vital information about the phase transitions which might have occurred in the early universe. The universe was filled with QGP phase during the first $10\mu s$ after the Big Bang evolution, which is understood to be a dilute gas of weakly coupled quarks and gluons. Due to expansion of the universe, the temperature decreased and the QGP turned into neutrons and protons, which further formed the atomic nuclei. QGP may occur naturally under high baryon number density and relatively low temperature, in astrophysical compact

objects like neutron stars. Broad research programs of the heavy-ion collision experiments like the Relativistic Heavy Ion Collider (RHIC) at the Brookhaven National Laboratory (BNL) and the Large Hadron Collider (LHC) at European Center for Particle Physics (CERN) are still going on to produce the QGP in the terrestrial laboratory conditions.

1.2 The Phases of QCD

The phase transition from the hadronic matter to QGP can be represented on the phase diagram of QCD. We are engaged in a exploration of the QCD phase diagram as a function of temperature T and baryon number chemical potential μ (Fig.1.1). Because of asymptotic freedom, at high temperature and/or high baryon density, the phase of QCD is described in terms of quarks and gluons degrees of freedom, rather than hadrons. At sufficiently high temperature $T >> \Lambda_{QCD}$ (Λ_{QCD} is the QCD scaling factor), the system is made up of weakly interacting quarks and gluons. Most of the information in such a system is based on the descriptions of perturbation theory. To study the transition region, where the hadronic description is no longer valid and perturbation theory is not yet feasible due to the large QCD coupling, one needs to take into account the non-perturbative nature of QCD.

The early Universe extremely expanded and cooled down and matter underwent a series of symmetry-breaking phase transitions. The study of phase transition from QGP to hadrons in the early Universe has a long history. The color deconfined QGP cools down below critical temperature T_c and comes to a color confined hadron system.

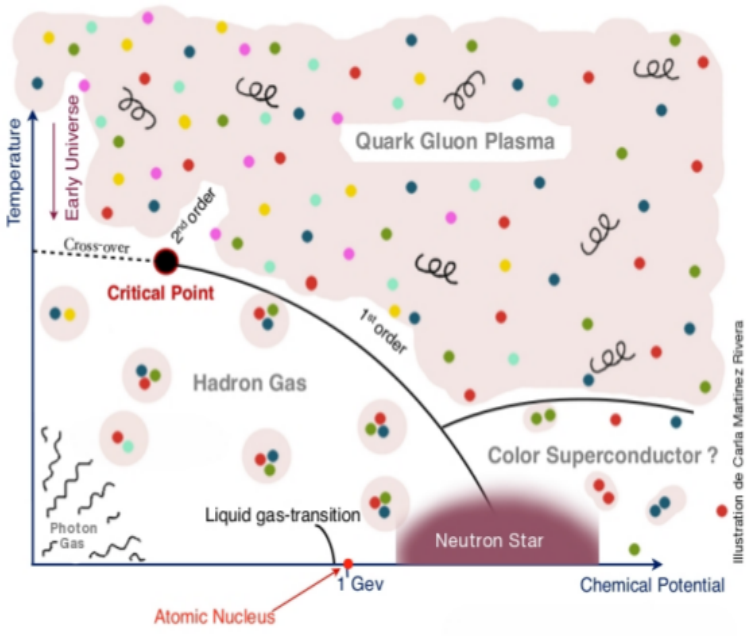

Figure 1.1: QCD Phase Diagram

1.3 Asymptotic Freedom and Confinement in QCD

QCD is the field theory of quarks and gluons. In QCD, hadrons are composed of elementary quarks and gluons, which are confined by the strong force. While comparing with other three fundamental interactions it is the strongest as the name suggests. Quarks, also called flavors, carry a non-Abelian color charge which is a three dimensional vector. Strong interaction among quarks is mediated by gluons.

Asymptotic freedom in QCD states that, the interaction strength α_s between quarks becomes smaller at short distance scale. In these condition the quarks and gluons interact weakly and they are almost free. The asymptotic freedom was first proposed by Gross and Wilczek, and Politzer [1, 2], which was recognised with the award of Nobel prize in 2004.

We can explain asymptotic freedom by recalling force between two electric charges in quantum electrodynamics (QED). Consider that the two electric

charges are screened by electric charge present in the vicinity (submerged in a medium with dieletric constant $\epsilon > 1$). In the quantum field theory (QFT), vacuum is understood as the lowest energy state of a field system and is filled with negative energies. When a photon passes through the vacuum, induced transitions of an electron from negative to positive energy states occurs, forming a virtual electron-positron pair, known as vacuum fluctuation, shown in the first diagram of Fig.1.4. The force between two electrons in vacuum is in the form,

$$F = \frac{\alpha_e(r)}{r^2}, \tag{1.1}$$

where α_e is the effective fine structure constant. It depends on the momentum transfer $q \approx 1/r$. In the limit $r \to \infty$, $q \to 0$, the coupling strength become $\alpha_e(q = 0) = 1/137$. In QED, the dependence of the fine structure constant on the momentum transfer can be express as,

$$\mu \frac{d\alpha(\mu)}{d\mu} = \beta(\alpha(\mu)), \tag{1.2}$$

where the momentum scale μ corresponds to $1/r$. The β function at the lowest order is,

$$\beta(\alpha_e) = \frac{2\alpha_e^2}{3\pi}. \tag{1.3}$$

The solution is,

$$\alpha_e(\mu) = \frac{\alpha_e(\mu_0)}{1 - \beta \ln(\frac{\mu^2}{\mu_0^2})}. \tag{1.4}$$

From the above relation it is clear that, interaction strength of the two electrons gets stronger as the distance between them become smaller. i.e, QED becomes a strongly-coupled theory at very short distance scale.

QCD also takes the above differential equation Eq.(1.2) for the strong cou-

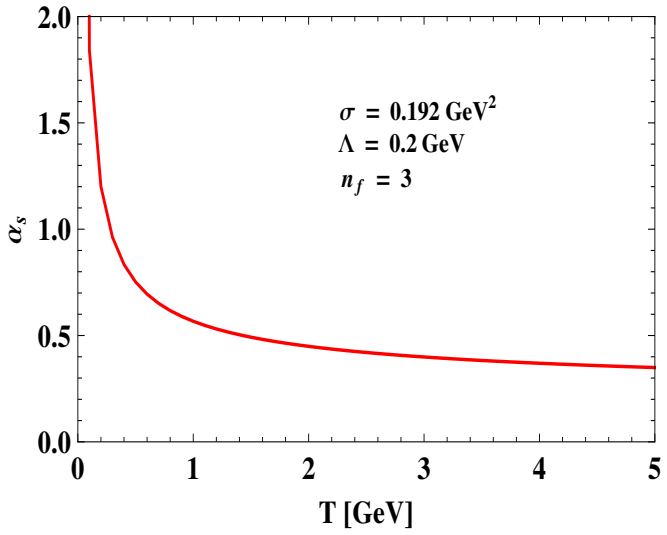

Figure 1.2: The QCD coupling constant as a function of temperature.

pling constant, but the β function has a different form as given below,

$$\beta(\alpha_s) = -\frac{\beta_0}{6\pi}\alpha_s^2 - ... \tag{1.5}$$

After solving the differential equation (1.2), the coupling constant to lowest order is given by [3],

$$\alpha_s(\mu) = \frac{12\pi}{(33 - 2n_f)\ln(\frac{\mu^2}{\Lambda^2_{QCD}})}, \tag{1.6}$$

where n_f is the number of active quark flavor and Λ_{QCD} is the QCD scale parameter. α_s goes to zero as the momentum scale $\mu \to \infty$ (the distance approaches zero), called asymptotic freedom. This behaviour of the strong coupling constant α_s is shown in Fig.1.2.

At large momentum transfer strongly interacting systems can be studied using perturbation theory. At finite temperatures or at equivalent high energies, strength of the interaction decreases sufficiently to allow the constituents to behave as free particles. The partons (color charges) are not confined in this regime and act similar to an electric charge. This justifies the usage of theoretical models. QCD is a well understood and tested theory in the high energy regime,

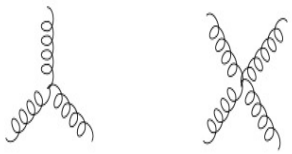

Figure 1.3: Self-interactions of gluons, three and four gluon self-interactions.

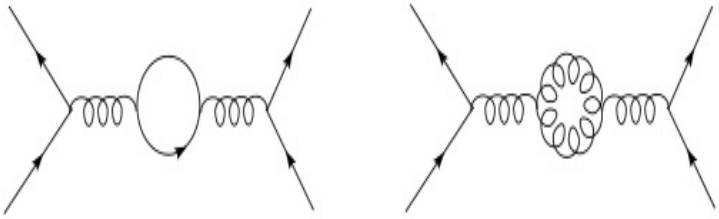

Figure 1.4: Screening and anti-screening in QCD.

but in the low energy regime and in the transition to the low energy regime, one has to use non-perturbative approaches like phenomenological models and lattice QCD. The QCD scale parameter sets the scale at which the coupling constant becomes large and the physics becomes non-perturbative.

No free quarks are seen in nature, they interact with each other through the gauge potentials and carry energy and momentum themselves. The interactions of eight gluons do not come in as a simple repetition of the photon interaction in QED. They have the property of gluon self-interactions, as shown Fig.1.3. The second diagram in Fig.1.4 represents the interaction among gluons leading to anti-screening effect, which makes the coupling stronger at large distances. The self-interactions of colored gluons provide insight into the differences between QCD and QED and it is responsible for many of the salient features of QCD.

The strongly interacting system at zero temperature is a color singlet at distance scale larger than $1/\Lambda_{QCD}$. Hence, the isolated free quarks cannot exist in nature. This effect is called quark confinement. The color confinement of QCD is a theoretical idea which is consistent with experimental results. The interaction between quark-antiquark pair gets stronger as the distance between

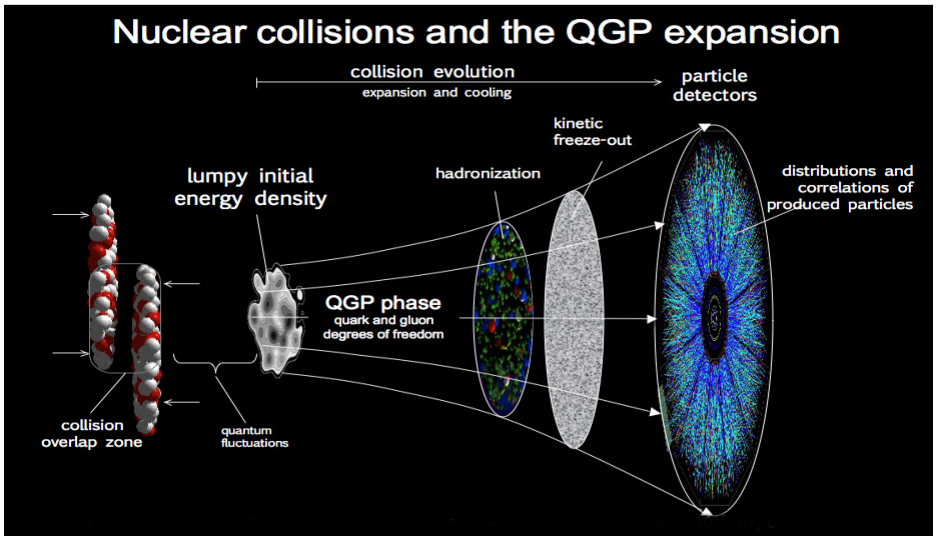

Figure 1.5: The nuclear collision in laboratory and QGP expansion (Source: Paul Sorensen - BNL).

them increases. The concept of confinement can be explained using the analogy of stretched spring, which when stretched beyond the elastic limit, breaks and produces two springs. In the case of the quark-antiquark pair, a part of the stretching energy goes into the creation of the new quark-antiquark pair when it is pulled beyond a certain distance. Hence one cannot see a free quark.

1.4 Experiments at BNL and CERN

The experiments at the CERN and BNL have been exploring the existence of QGP by colliding nuclei at relativistic energies. A pictorial depiction of the nuclear collision and QGP expansion is given in Fig. 1.5.

A summary of different heavy-ion collision experiments with different beam energies is given in Table 1.1, which probe different regions of the QCD phase diagram.

The first experimental verification of the deconfinement phase transition was reported in SPS[1], CERN, having center of mass energy $\sqrt{s_{NN}} = 17GeV$ for Pb+Pb collisions, with the chemical potential, $\mu_B \approx 250MeV$. Here, the freeze-

[1]SPS- Super Proton Synchrotron is a particle accelerator at CERN

Table 1.1: Energy of nuclear collision experiments with center of mass energies

Accelerator	Laboratory	Colliding Ions	$\sqrt{S_{NN}}(GeV/A)$	started Year
AGS	BNL New York	$Si^{28} + Au^{197}$	5	1986
SPS	CERN Geneva	$S^{32} + Pb^{208}$	19	1986
AGS	BNL New York	$Au^{197} + Au^{197}$	5	1992
SPS	CERN Geneva	$Pb^{208} + Pb^{208}$	17	1994
RHIC	BNL New York	$Au^{197} + Au^{197}$	200	2000
LHC	CERN Geneva	$Pb^{208} + Pb^{208}$	5500	2008

out temperature is about $T_c \approx 170MeV$, it compares fairly well with the critical temperature predicted by the lattice QCD calculations. The SPS experiments reported several important signatures of the phase tranisition, like strangeness enhancement, charmonia suppression etc., which can be explained as due to the formation of QGP.

In 2005, RHIC at BNL announced [4] an important discovery of deconfined state of matter, i.e, the strongly interacting QGP (sQGP), and that it behaves like a 'perfect liquid'. Hence these results from RHIC differ significantly from the theoretical predictions of QGP which consider QGP as an 'ideal gas'. The key signatures attributed to the existence of QGP at RHIC energies is the jet quenching in head-on Au+Au collisions. The observation of larger elliptic flow at RHIC energies, suggestive of the existence of partonic degrees of freedom in the created medium.

1.5 Lattice QCD

Lattice QCD (lQCD) is a non-perturbative approach to QCD. Lattice gauge theory was proposed by G. Wilson in 1974 [5]. Through this approach, we can study the strongly coupled system. Here the field degrees of freedom are discretized on a four-dimensional space-time lattice grid. Inorder to explain QGP equilibrium phases and the phase transitions, we need to study the framework of non-perturbative treatment of QCD on discrete lattice of space-time coordinates.

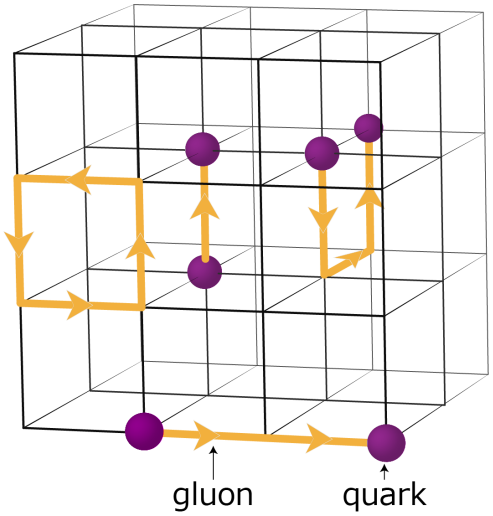

Figure 1.6: Lattice QCD.

In weakly interacting system, the coupling constant is small and perturbation theory become reliable. When the coupling constant is of order unity or at region of small momentum transfer, perturbative methods become failure, in this domain lattice QCD provides a non-perturbative tool from first principles. Lattice QCD also addresses the issues like the quark confinement [6], chiral symmetry breaking [7] and the equilibrium properties of QCD at finite temperature [8].

In lattice QCD [9], Euclidean space-time is discretised (lattice regularized QCD), usually on a hyper-cubic lattice with lattice spacing a. The quark fields are placed on sites and gauge fields on the links between sites as shown in Fig.1.6. We take the limit of vanishing lattice spacing and treat QCD as a continuum theory. Actually it is a tuning of bare coupling constant to zero according to the renormalization group. Lattice QCD allows non-perturbative calculations by numerical evaluation of the path integral that defines the proposed theory. Practical Lattice QCD results come with the use of available computational resources and the efficient algorithms.

Table 1.2: Quark mass evaluation range of the Particle Data Group (2012) [14]

Quarks	Symbol	Mass evaluation range
Up	u	2.3 ± 0.7 MeV
Down	d	4.8 ± 0.5 MeV
Strange	s	95 ± 5 MeV
Charm	c	1275 ± 25 MeV
Bottom	b	4180 ± 30 MeV
Top	t	173210 ± 510 MeV

1.6 The QGP Signatures

The evidence for QGP generation in heavy-ion collisions has appeared to be difficult to comprehend. The mixture of Quarks and gluons coexisting in the QGP state cannot be measured directly. The signals of QGP are mixed with the particles produced by final state hadronisation. A description of the concept, that are sensitive to the properties of plasma, needed to find the promising signature of QGP.

1.6.1 Quarkonium Dissociation Studies

Quarkonium is a bound state of a heavy quark Q and its anti-quark $\bar{Q}$ pair. The heavy masses of the charm (c) and bottom (b) quarks compared to the light (u, d, s) quarks (see table 1.2), provide heavy quarkonia with properties that differ significantly from those of the light mesons. The charmonium is the bound state of charm and anti-charm ($c\bar{c}$) quark pair, corresponding bottom and anti-bottom ($b\bar{b}$) quark pair is known as bottomonium. The top (t) quark decays via the weak interaction on a time scale below that associated with quarkonium formation, so that quarkonia composed of top anti-top ($t\bar{t}$) quark pairs have not seen [10].

Quarkonia are considered as the fingerprint in the formation of QGP. The J/ψ and $\Upsilon(1S)$ states of charmonium and bottomonium, respectively, dissociates at high temperature, whereas the resonance state of charmonium (χ_c, $\psi(2S)$) and those of bottomonium (χ_b, $\Upsilon(2S)$ and $\Upsilon(3S)$) dissociates at low temperature.

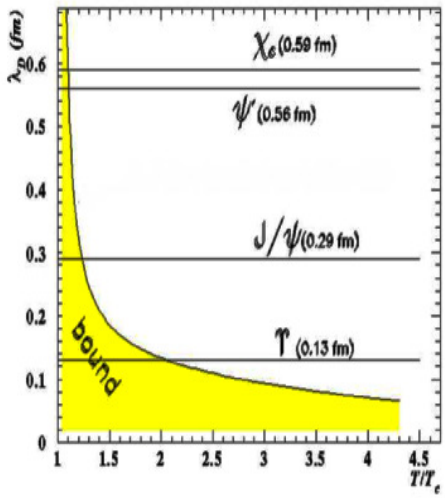

Figure 1.7: Debye screening length for different quarkonia states as a function of T/T_c.

The quarkonium production in heavy-ion collisions has already been addressed by the RHIC and LHC experiments. The screening effect of quark and antiquark will lead to the suppression of quarkonia, which has been suggested as a signature for QGP [11]. In the QGP phase the interaction potential would be screened beyond a Debye screening length, λ_D. The interactions between quarks and antiquarks get weakened exponentially beyond Debye screening length. When the quarkonium dimension becomes larger than λ_D , dissociation of quark and antiquark pairs take place, as shown in Fig.1.7.

The experimental evidences of the NA50 Collaboration [12] also shows the anomalous J/ψ suppression in Pb+Pb collisions. The phenomenon of anomalous J/ψ suppression has been subject to a detailed investigation by M. Nardi et al in [13].

1.6.2 Strangeness Enhancement Studies

The strangeness content is enhanced to a greater extent in a hadron to quark-gluon plasma phase transition. Due to the restoration of chiral symmetry, the probability for the production of multi-strange hyperons will also be greatly enhanced [12]. The WA97 Collaboration [13] observed the enhanced production

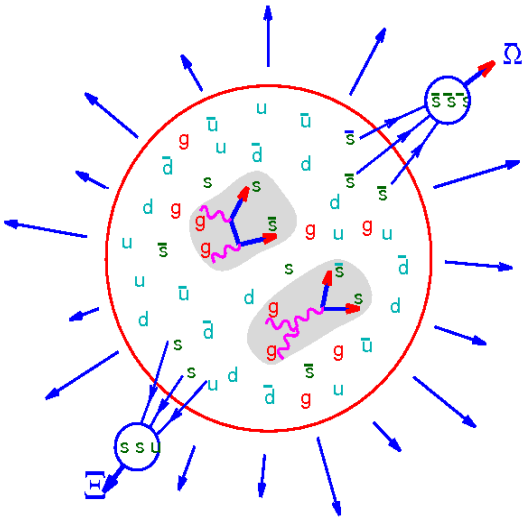

Figure 1.8: Strangeness enhancement (Source: Johann Rafelski, lecture series).

of multi-strange hyperons, in particular production of Ω^- and $\bar{\Omega}^+$ in $Pb + Pb$ collisions at $158AGeV$.

Multi-strange hyperons, formed by the collision of the produced pions with nucleons, leads to the enhancement of kaons and Λ particles. The secondary collisions of kaons in the medium with a Λ particle can raise the strangeness of the hyperon. These collisions increase with increase in the size of the colliding nuclei. The discrepancies in the yields of the Ω hyperons with the theoretical relativistic quantum molecular dynamics model (RQMD cascade model) calculations [17] may be an additional evidence for the production of the quark-gluon plasma in Pb+Pb collisions.

The abundance of strange quarks gradually leads to the formation of a chain of rescattering processes. The high density of strangeness at the time of QGP hadronization is a natural source of multi-strange hadrons.

In the QGP, production of strange quarks and their antiparticles predominantly occur through,

1) Collision of light quarks u and d and its antiquarks

$$q + \bar{q} \rightarrow s + \bar{s}. \tag{1.7}$$

2) Fusion of two gluons

$$g + \bar{g} \rightarrow s + \bar{s}. \tag{1.8}$$

1.6.3 Direct Photon Production

When matter undergoes a phase transition from QGP to the hadron system, photons will arise from the electromagnetic interaction of the constituents of the plasma. It will provide vital information on the properties of the QGP at the time of their emission, because photons are hardly absorbed by the medium. E. Shuryak et al., [18, 19] explain how photons in high-energy heavy-ion collisions become an evidence for the production of QGP. The main source of production of direct photons in the QGP medium are,

(1) Annihilation Process

$$q + \bar{q} \rightarrow \gamma + g. \tag{1.9}$$

(2) QCD Compton scattering

$$g + q \rightarrow \gamma + q. \tag{1.10}$$

$$g + \bar{q} \rightarrow \gamma + \bar{q}. \tag{1.11}$$

The measurement of direct photons from electromagnetic interaction of the constituents of the QGP is a laborious task, because an abundance of photons are produced during the decay of π^0 and μ^0 in heavy ion collision. Many meaningful literature have been developed [20] for the subtraction of photons from the π^0 and μ^0 background to obtain direct photons, as shown in Fig. 1.9.

Photon transverse momentum p_T must be greater than $2GeV/c$ to minimize the contributions of photon from the hadron phase. In the hot QGP, photons have p_T in the range of $2 - 3GeV/c$ [21]. Photons in this region of transverse momenta are also produced by the collision of constituents of the projectile

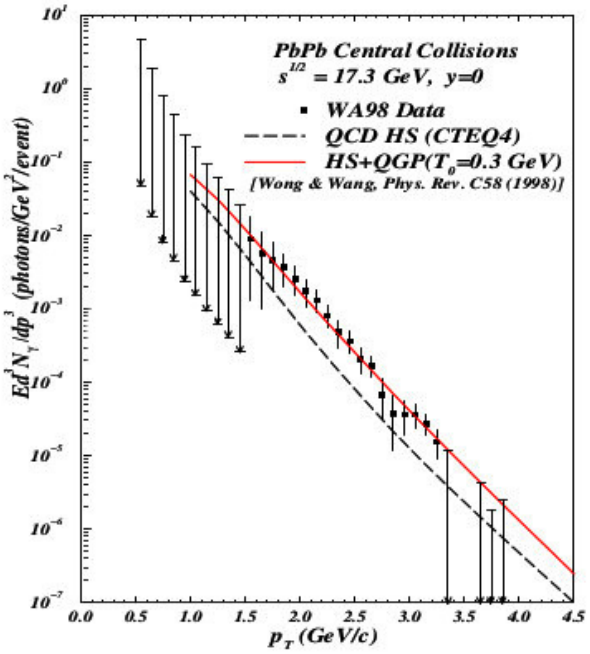

Figure 1.9: The spectrum of direct photons [20, 22].

nucleons with constituents of the target nucleons. In order to infer the net photons from the QGP, the contribution from other sources must be subtracted.

1.6.4 Di-lepton Production

In QGP, the quark and antiquark annihilate to create virtual photons which decay into lepton pairs L^+L^- (e^+e, $\mu^+\mu$), termed as dilepton, as shown in Fig. (1.10(a)). The dilepton production can also take place via Drell- Yan process Fig. 1.10(b) as well as by decays of hadron resonances Fig. 1.10(c).

After creation, dilepton pass through the collision region to the particle detectors without any further collisions, thus providing undamaged information about the interiors of the fireball. The effects of medium will change the quark dispersion relation in QGP in such a way that sharp gaps arise in the production rate of low mass dileptons. This is the unique signature for the presence of deconfinement. The dilepton invariant mass is,

$$M^2 = (P_L^+ + P_L^-)^2, \tag{1.12}$$

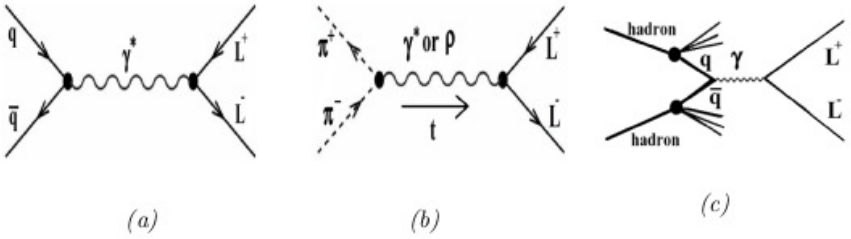

Figure 1.10: Reaction mechanisms for the production of dilepton.

where P_L^+ and P_L^- are the four-momenta of the dilepton. The dilepton's transverse momentum is,

$$p_T = (p_L^+)_T + (p_L^-)_T, \tag{1.13}$$

where $(p_L^+)_T$ and $(p_L^-)_T$ are the transverse momenta of the dilepton.

1.6.5 Jet Quenching

The relativistic heavy ion collision of partons in the colliding hadrons produces various other partons with very high transverse momenta, which fly off to all possible directions and finally fragment into narrow cones of hadrons called jets. When the jet partons propagate through the hot and dense medium, they interact with the particles of the medium, undergoing multiple scattering and loose energy and momenta before hadronizing. The resulting attenuation of the jet parton due to energy loss in the dense medium is called 'jet quenching'. This loss is observed through the nuclear modification factor, R_{AA}, given by,

$$R_{AA}(p_T, b) = \frac{\frac{dN_{AA}}{d^2p_T dy}}{T_{AA}(b)\left[\frac{d\sigma_{pp}}{d^2p_T dy}\right]}. \tag{1.14}$$

The numerator of this modification factor is a single particle transverse momentum distribution of a jet parton, produced in nucleus-nucleus collision and traveling through thermal medium. The denominator part has single particle

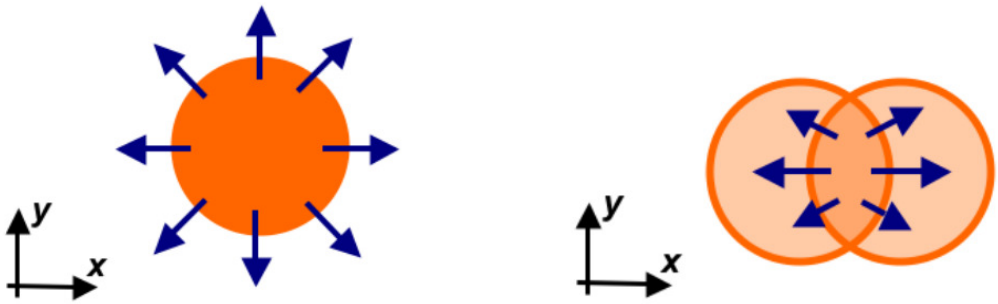

Figure 1.11: Radial flow and elliptical flow.

distribution of the jet parton, produced in proton-proton collision. $T_{AA}(b)$ is the nuclear thickness function, which is a proton to nucleus scaling factor and is a function of impact parameter b. This idea was fist proposed by Bjorken [23]. It shows that jet particle traveling inside a bulk partonic matter must loose a significant part of its energy before hadronizing. If the ratio tends to be less than unity, it is the definite measure for jet suppression in the medium [24] - [26]. It was one of the first proposed signatures of QGP formation in relativistic heavy-ion collisions.

1.6.6 Anisotropic Flow

Anisotropic flow is an important observable in relativistic heavy-ion collisions, because it provides information about the thermodynamics and collective properties of the hot and dense environment formed in the early universe. Anisotropic particle distributions were first proposed as a signal of collective flow in ultra-relativistic heavy-ion collisions. For the non-central heavy ion collisions, the azimuthal momentum anisotropy can be explained in terms of the fourier expansion given by,

$$E\frac{d^3N}{d^3p} = \frac{d^2N}{2\pi p_T dp_T dy}\left[1 + \sum_{n=1}^{\infty} 2v_n \cos\left[n(\phi - \psi)\right]\right], \tag{1.15}$$

where v_n is the Fourier or flow coefficients, ϕ is the azimuthal angle of the particle and ψ is the azimuthal angle of the reaction plane in the laboratory frame.

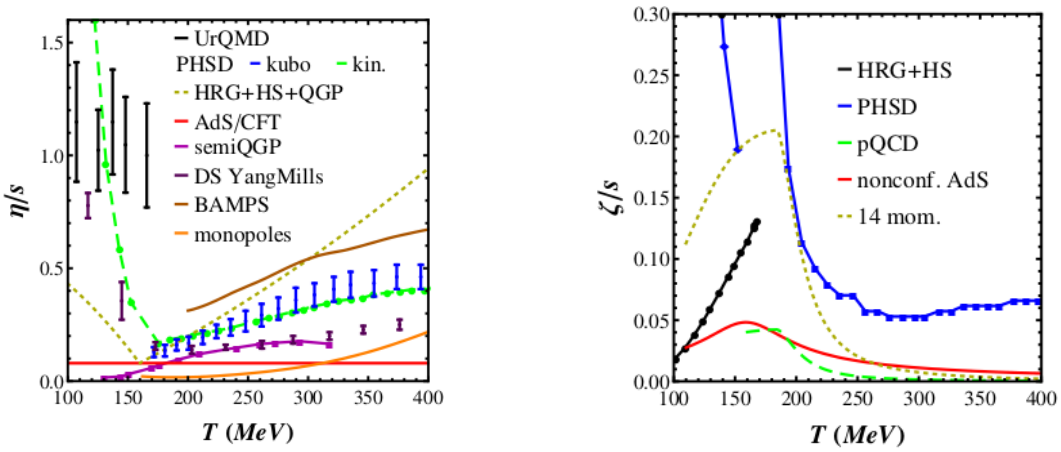

Figure 1.12: η/s and ζ/s for various temperature range (Source: http://arxiv.org/abs/1512.06315v1).

The first Fourier coefficient, $v_1 =< \cos(\phi) >$ corresponds to the strength of the directed flow and the second coefficient $v_2 =< cos(2\phi) >$ quantifies the strength of the elliptic flow. These two flows illustrated in Fig. 1.11. The magnitude of v_2 is sensitive to the initial conditions and equation of state of the hot and dense fireball. The higher order flow coefficients such as v_3 , v_4 , v_5 etc. are the parameters for studying initial state fluctuations and to obtain ratio of shear viscosity to entropy density (η/s) of the hot fluid produced in a collision.

1.7 Transport Coefficients of QGP

Elliptic flow is one of the important evidences for the existence of QGP. After initial stage of heavy ion collisions, interacting system reaches a local thermal equilibrium, and the pressure gradients arise. The pressure gradients are steeper along the direction of impact parameter and lead to azimuthal momentum space anisotropy of particle emission, which is defined as elliptic flow.

The shear viscosity and bulk viscosity in heavy ion collisions have significantly affected the elliptic flow 'v_2' and higher order Fourier coefficients. Shear viscosity acts as resistance against the deformation of a fluid element, whereas the bulk viscosity acts against the expansion or compression of the fluid.

Various theoretical results suggest that, near the QCD critical temperature T_c, the behaviour of transport coefficients such as ratio of shear viscosity to entropy density (η/s) is suppressed and the ratio of bulk viscosity to entropy density (ζ/s) is strongly enhanced, as shown in Fig. (1.12). The η/s has an influential role in the dynamical flow behaviour of the medium, hence on the elliptic flow parameter v_2 after freezeout. Experimental measurements of this parameter suggest a value of η/s of the order of 0.12 at RHIC and 0.2 at LHC energies [27]. Even at larger couplings found in LHC than those found at RHIC the limit of $1/4\pi \approx 0.08$ from AdS/CFT might actually be reachable. The systematic uncertainties caused by the known magnetic field effects or large fluctuations in the initial state may vary the measurements of the value η/s. To find consistency between experiment and theoretical results, one also needs predictions from AdS/CFT ($1/4\pi \approx 0.08$) with finite coupling corrections.

1.8 A Brief History of Theoretical Models on QGP

The study about the characteristics of QGP is mainly based on: (1) QCD calculations on the lattice (lQCD), (2) the perturbative regime (pQCD), (3) theoretical and phenomenological models.

1.8.1 MIT Bag Model

The first idea of the bag model appeared in 1967 [28]. This model framed of three massless quarks in a vacuum cavity of radius R with square well potential. In I974, a group of scientists from the Massachussets Institute of Technology (MIT) modified the Bag model [29]. Now it is termed as MIT Bag model. In this model, quarks are treated as massless particles inside a bag of finite dimension and infinitely massive, outside the bag. Confinement in the model is the result of balance of the inward bag pressure B, and the stress arising from the quark

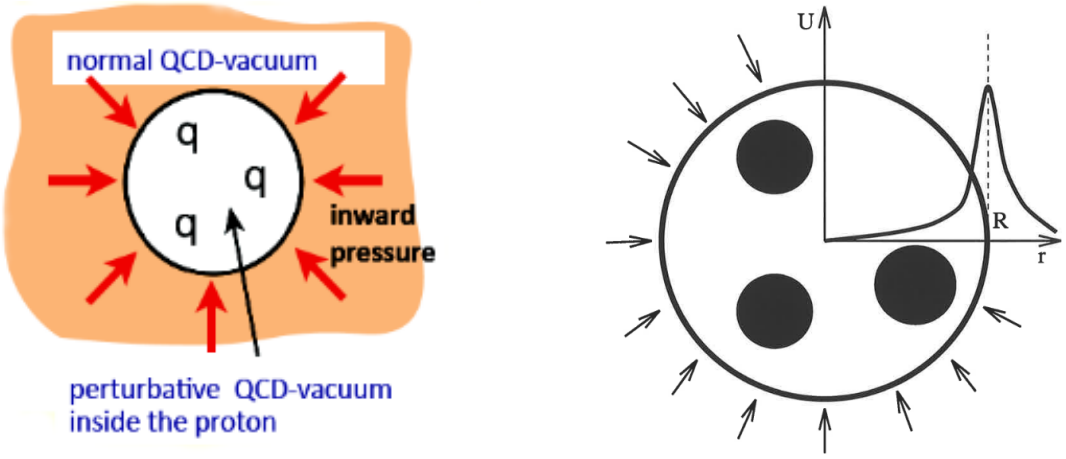

Figure 1.13: Bag model.

kinetic energy. The parameter B is the bag pressure which take into account the nonperturbative effects of QCD ($B \approx 200 MeV/fm^3$). A pictorial representation of the Bag model is given in Fig.1.13. In the MIT model, partons move freely inside the 'Bag' and the phase transition can be formed by compressing the bags against each other. Under high baryon number and energy densities, the quarks and gluons are free to move through large spatial regions. The pressure in terms of Bag constant is,

$$P = \frac{37\pi^2}{90} T^4 - B(T). \tag{1.16}$$

The energy density,

$$\epsilon = \frac{37\pi^2}{30} T^4 + B(T). \tag{1.17}$$

The Bag pictures in QGP and hadron gas separately can throw some light on the phase transition and its critical parameters. But it is unrealistic, because in this model the QGP contained in a big bag with a bag pressure B, hence one cannot construct a first order phase transition. Similarly in a hot and dense hadron gas, the interactions are intense and strong in magnitude.

1.8.2 The Strongly Interacting Quark-Gluon Plasma Model (sQGP)

The present theoretical developments predict the strongly interacting behaviour of the QGP produced at RHIC. The experiments and lattice simulations show different properties at temperatures of the order of a few times the critical temperature T_c, ranging from 1 to $3T_c$, in this range QGP displays strong interaction between the constituents. In sQGP model [30] a theory was developed to address the properties of a large number of binary bound states at $T > T_c$, consisting of both colorless (hadronlike) and colored (exotic) bound pairs of gq, qq, and gg. The binding energies and zero-binding lines on the phase diagram were evaluated and their contribution to pressure was estimated.

1.8.3 The Strongly Coupled Quark-Gluon Plasma Model (SCQGP)

The QGP near transition temperature T_c is called the strongly coupled system [4]. At high temperature QGP is a quasi colour neutral gas of charged and neutral particles which exhibits collective behaviour as in the QED plasma. In QGP, collective effects of colour neutral objects like hadrons and glue balls must be negligibly small in number. In QED the recombination and ionization are possible at the same rate. The same is not possible in deconfined state such as QGP.

In strongly coupled plasma (SCP), at high temperature, the system is in ionized state and there is a negligibly small amount of neutral atoms. Similarly in SCQGP, there may be negligibly small hadrons due to Coulomb binding interactions, but there are no confinement interactions. In the phenomenological model for SCQGP, the author [31] derived a modified equation for energy density by including relativistic and quantum effects as,

$$\epsilon = (2.7 + U_{ex}(\Gamma))nT. \tag{1.18}$$

Taking $n = 1.1a_f T^3$ and $\epsilon_s = 3a_f T^4$ for ideal EoS for massless relativistic gas.

The plasma parameter Γ defined as the ratio of average potential energy to average kinetic energy of the particles for SCQGP and is given by

$$\Gamma = \frac{< P.E >}{< K.E >} = \left(\frac{4.4\pi a_f}{3}\right)^{1/3} \frac{g_c}{2}\alpha_s(T). \tag{1.19}$$

In SCP $g_c = 1$ and in SCQGP it is different for gluon plasma and flavoured QGP. a_f is a constant which depends on degrees of freedom and is given by,

$$a_f = (16 + \frac{21n_f}{2})\frac{\pi^2}{90}. \tag{1.20}$$

The coupling constant $\alpha_s = 1/137$ in SCP, but for SCQGP by inclusion of quantum effects α_s for single loop order becomes,

$$\alpha_s(T) = \frac{12\pi}{(33 - 2n_f)\ln(\frac{T}{\Lambda_T})}, \tag{1.21}$$

where n_f is the number of flavours and Λ is the QCD scale parameter.

The pressure P for SCQGP can be derived using the relation $\epsilon = T\frac{\partial P}{\partial T} - P$. In SCQGP phenomenological model, QGP near and above $T = T_c$ is treated as a strongly coupled system. Thus an equation of state can be obtained via appropriate modifications of QED to take into account the colour and flavour degrees of freedom and quantum effects.

1.8.4 The Quasi-particle QGP Model (qQGP)

The qQGP is a phenomenological model, which treats the interacting massless quarks and gluons as non-interacting massive particles. To describe the non-ideal behaviour of QGP from lattice gauge theory (LGT) simulation of QCD [32], Satz et al.[33] and Peshier et al.[34] independently proposed quasiparticle picture of QGP. In the work of Peshier et al. on gluon plasma all thermodynamic quantities

were derived from the partition function,

$$\frac{PV}{T} = -\sum_{k=0}^{\infty} \ln(1 - e^{-\beta\epsilon_k}) \tag{1.22}$$

The single particle energy ϵ_k of quasi-gluon in terms of temperature dependent mass is,

$$\epsilon_k = \sqrt{k^2 + m^2(T)}, \tag{1.23}$$

where k is the momentum and $m(T)$ is the temperature dependent mass. β is defined as $1/T$. The expression for pressure can be denoted as P_{id}, similar to that of ideal gas with temperature dependent mass.

The thermodynamic inconsistency of the proposed quasiparticle model was identified in [35, 36] and remedied by introducing a temperature dependent vacuum energy. The idea was taken from the bag model of hadron spectroscopy and introduced the bag pressure term $B(T)$ in the expression for pressure,

$$P = P_{id} - B(T). \tag{1.24}$$

The corresponding energy density is,

$$\epsilon = \epsilon_{id} + B(T). \tag{1.25}$$

In the above mentioned literature different authors have exploited $B(T)$ in terms of temperature dependent bag pressure, vacuum pressure, residual interaction energy, etc and have derived the thermodynamic consistent relation for pressure and energy density. Different versions of quasi-particle models claim to explain lattice results either by adjusting free parameters in the model or by taking lattice results of the thermodynamic quantities and predicting all other thermodynamics.

There are quasiparticle models which do not involve extra terms like $B(T)$.

V. M. Bannur has been demonstrated that the thermodynamically consistent formulation of quasi-particle models is possible without the need for extra terms like $B(T)$ [37]. It has been shown that, all thermodynamic quantities can be derived in a consistent manner, starting with the expressions for energy density and number density, without any need for reformulation of statistical mechanics. In these models, it has been maintained that, the whole thermal energy is used to excite the quasiparticles [38, 39]. Such models have been able to obtain very good results in good agreement with the lattice data.

1.8.5 The Cornell Potential Model

The effective potential between a heavy quark and antiquark can be taken as the Coulomb-plus-linear potential, known as the Cornell potential. In the context of meson spectroscopy which is used to describe systems of quark and antiquark bound states, the Cornell potential model shows considerable success. The Cornell potential includes short distance color Coulombic interaction of quarks, which is mediated by a single gluon exchange, and the large distance confinement that arises from the color field flux tube between the quarks, via the linear term in a simple form. Cornell potential is expressed as,

$$V(r) = \sigma r - \frac{\alpha}{r}, \tag{1.26}$$

where α, σ are the strong coupling constant and string tension respectively. The first term which is analogous to the Coulomb potential in the QED is associated with scattering of the quark-antiquark pair inside the meson. The linear confinement comes from the strong-coupling expansion of the Wilson loop in lattice gauge theory with static quarks.

In [40], the Cornell potential model was used to derive EoS for QGP based on Mayer's theory of plasma [41]. The results were compared with the lattice QCD results of the gluon plasma. Later the EoS was extended to quark-antiquark plasma by Udayanandan et al. [42] and the results were compared with 2-flavour

and 3-flavour lattice QCD results. Here the cluster integral takes into account the interaction between the quarks and gluons, i.e, Cornell potential. This Cornell potential model has been successful in describing the spectra for both charmonia and bottomonia [43]. Sheikholeslami-Sabzevari [44] has obtained an EoS and found analytically the temperature at which the quarkonia suppression takes place using the modified Cornell potential. Furthermore, the screened potential models have been applied to calculate the heavy quarkonium spectrum [45], as well as the spectra of light hadrons [46]. In [47] the extended Simpson's rule has been used to solve the Schrodinger equation in momentum space with the screened Cornell potential. In this thesis we employ Cornell potential as the interaction potential between the partons under the mathematical framework of cluster expansion method.

In this thesis we studied quarkonia suppression and strangeness enhancement in QGP with Cornell potential, based on Mayer's cluster expansion method. The phase transition from QGP to Hadron system is investigated by considering the high density limitation of the Mayer's method of cluster expansion. The work has been extended by considering the modified Cornell potential and calculating the transport coefficients such as shear viscosity to entropy density ratio η/s and bulk viscosity to entropy density ratio ζ/s. We adopted the cluster expansion theory of plasma with proper modifications and compared this result with the results of lattice QCD. Finally we revisited the Cornell potential model and derived a modified EoS of QGP using CE method. Quantum effects near the transition temperature was included by considering bound states of light quarks and gluons in the strongly coupled regime. Good fit with the lattice QCD results was observed.

Bibliography

[1] David. J. Gross, Rev. Mod. Phys, Vol 77, No.3 (2005).

[2] H. David Politzer, Nobel Lecture, December 8 (2004).

[3] W. Greiner er al., Quantum chromodynamics, Springer (2007).

[4] J Adams et al. (STAR Collaboration), Nucl. Phys. A 757, 102 (2005).

[5] G. Wilson, Phys. Rev.D 10 , 2445 (1974).

[6] Martin Luscher, Ann.Henri Poincare, 4, 197 (2003).

[7] L. Giusti, M. Luscher, JHEP, 03, 013 (2009).

[8] E. Learman, Nuclear Physics A, 610, 12 (1996).

[9] M. Tanabashi et al., Phys. Rev. D, 98, 030001 (2018).

[10] Andrew Chisholm, Measurements of the X_c and X_b Quarkonium States in pp Collisions with the ATLAS Experiment, Springer, Switzerland (2015).

[11] T. Matsui and H. Satz, Phys. Lett. B 178 ,416 (1986).

[12] M. C. Abreu et al., Phys. Lett. B 477, 28 (2000).

[13] M. Nardi and H. Satz, Phys. Lett. B 442, 14 (1998).

[14] J. Beringer et al. (Particle Data Group), Phys. Rev. D, 86, 010001 (2012).

[15] J. Rafelski, Phys. Rep. 88, 331 (1982).

[16] WA97 Collaboration, E. Andersen et al., Phys. Lett. B 449, 401 (1999).

[17] H. Sorge, Phys. Rev. C 52, 3291 (1995).

[18] E. L. Feinberg, Nuo. Cim., 34, 391 (1976).

[19] E. Shuryak, Phys. Lett. B 78, 150 (1978).

[20] WA98 Collaboration, M. M. Aggarwal et al., Preprint "Direct Photon Production in 158A GeV 208 Pb + 208 Pb Collisions".

[21] J. Kapusta, P. Lichard, and D. Seibert, Phys. Rev. D 44, 2774 (1991).

[22] C. Y. Wong and H. Wang, Phys. Rev. C 58, 376 (1998).

[23] J. D. Bjorken, Fermilab-Pub-82/59-THY, Batavia (1982).

[24] R. Karabowicz (BRAHMS Collaboration), Nucl. Phys. A 774, 477 (2006).

[25] A. Grelli (ALICE Collaboration), Nucl. Phys. A 904, 635c (2013).

[26] M. B. Tonjes (CMS Collaboration), Nucl. Phys. A 904, 713c (2013).

[27] Charles Gale et al., Phys.Rev.Lett., 110, 012302, (2013).

[28] P.N. Bogolioubov, Ann. Inst. Henry Poincaré 8, 163 (197a).

[29] A. Chodos et al., Phys. Rev.D9, 3471 (1974).

[30] Edward Shuryak and Ismail Zahed, Phys. Rev. D 70, 054507 (2004).

[31] Vishnu M Bannur, J. Phys. G: Nucl. Part. Phys. 32 ,993 (2006).

[32] D.H. Rischke et al., Phys. Lett. B 278, 19 (1992).

[33] V. Goloviznin, H. Satz, Z. Phys. C 57, 671 (1993).

[34] A. Peshier et al., Phys. Lett. B 337, 235 (1994).

[35] M.I. Gorenstein, S.N. Yang, Phys. Rev. D 52, 5206 (1995).

[36] A. Peshier, B. Kampfer and G. Soff, Phys. Rev. D66, 094003 (2002).

[37] V. M. Bannur, Physics Letters B 647, 271–274 (2007).

[38] V. M. Bannur, Eur. Phys. J. C 50, 629 (2007).

[39] V. M. Bannur, Physical Review C 78, 045206 (2008).

[40] V. M. Bannur, Phys. Lett B 362, 7-10 (1995).

[41] R Balescu, Statistical mechanics of charged Particles (Inter science Publishers, Inc., New York, 1963).

[42] K. M. Udayanandan, P. Sethumadhavan, and V. M. Bannur, Phys. Rev.C 76 , 044908 (2007).

[43] G. S. Bali, Phys. Rep. 343, 1 (2001).

[44] B. Sheikholeslami-Sabzevari, Phys. Rev. C 65, 054904 (2002).

[45] P. Gonzalez et al., Phys. Rev. D 68, 034007 (2003).

[46] J. Segovia, D. R. Entem, and F. Fernandez, Phys. Lett. B 662, 33 (2008).

[47] Jiao-Kai Chen, Phys. Rev. D 86, 036013 (2012).

Chapter 2

Studies of Quarkonium Dissociation and Multi-strange Hadronisation using Cluster Expansion Method

2.1 Introduction

The study of quarkonium dissociation has been considered as a possible signature for the occurrence of QGP in relativistic heavy ions collisions [1, 2]. On the footing of the Mayer's cluster expansion method [3, 4], a study has been performed and the criterion obtained for the temperature, where heavy quarkonium ($J/\psi(c,\bar{c})$ and $\Upsilon(b,\bar{b})$) suppression has already been obtained [5]. This finding, however, was based on grand canonical partition function of the system which ignored the limitations of the restrictive summation, $\sum_{l=1}^{N} lm_l = N$. The present study is based on canonical partition function of the system and helps to eliminate such deficiencies.

We intend to obtain an equation of state at which a non-ideal quark-antiquark plasma condenses into cluster of quarks, based on Mayer's cluster expansion method [3]. The EoS of quarkonia like charmonium ($J/\psi(c,\bar{c})$) and bottomonium ($\Upsilon(b,\bar{b})$) has been studied and the criterion for quarkonium dissociation

near the transition temperature T_c has been discussed. Strangeness enhancement is one of the important signatures of QGP [12, 13]. The collision of light quark and fusion of gluons are the natural source of strange particles. The clustering of these strange quarks in the phase transition region and hence the multi-strange hadronisation can be investigated via cluster expansion method. We have obtained EoS for $\Phi(s\bar{s})$ and $\Omega^{-}(sss)$ etc., and studied muti-strange hadronisation process. In order to calculate third cluster integral, we have made use of the bipolar coordinate integral [6]. The EoS has been studied using Cornell potential with the effect of screening [7, 8].

V.M.Bannur et al. had obtained an equation of state (EoS) for QGP using Cornell potential based on Mayer's theory of plasma [14, 15]. In the present work plasma is assumed to be homogeneous. We only consider the contribution of quarks and anti-quarks, since here the gluons are massless and interaction free. The equation of state is classical and non- relativistic, i.e. we consider the quarks to have mass equal to or greater than that of the strange quarks, so that the non- relativistic approximation can be applied. We should realize that, higher the temperature and mass, the smaller the thermal wavelength $\lambda_T = \sqrt{\frac{2\pi}{MT}}$ and we enter more and more the range of classical statistical mechanics [16].

2.2 Mayer's Cluster Expansion Method

Mayer and his collaborators introduced a method of expansions, in the case of real gases obeying classical statistics [3, 4]. In statistical physics, Cluster expansion method provides a systematic way of computing power series for thermodynamic potentials. Partition function includes the cluster of particles and the interaction within the clusters is governed by the short-range and pairwise additive potential, $U = \sum_{i<j}^{N} u(r_{ij})$, (shown in Fig 2.1), where r_{ij} is the distance between particle i and j. Then the partition function of the system is,

$$Q_N(V,T) = \frac{1}{N!\lambda^{3N}} \int \exp\left[-(\frac{1}{k_B T}) \sum_{i<j}^{N} U(r_{ij})\right] d^3r_1 ... d^3r_N = \frac{1}{N!\lambda^{3N}} Z_N(V,T),$$

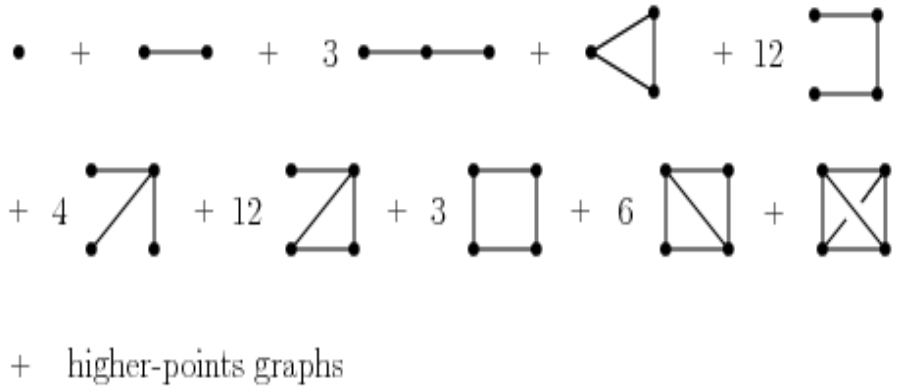

Figure 2.1: Mayer cluster expansion method.

(2.1)

where λ is the thermal wavelength of the particles, while $Z_N(V,T)$ stands for the configuration integral.

Mayer introduced a two particle function f_{ij} called Mayer f-function,

$$f_{ij} = f_{(r_{ij})} = e^{-\frac{U(r_{ij})}{k_B T}} - 1 \tag{2.2}$$

Mayer function in the case of Cornell potential and screened Cornell potential is depicted in Fig.2.2. The integrand exponent of the configuration integral can be expanded in the form,

$$\prod_{i<j}^{N}(1+f_{ij}) = 1+\sum_{i<j} f_{ij} + \sum_{i<j<k} f_{ij}f_{ik} + \sum_{i<j,k<m} f_{ij}f_{km} + \sum_{i<j<k} f_{ij}f_{ik}f_{jk} + ... \tag{2.3}$$

All independent integrals in the sum, for a group of N particles, can be collected into the Cluster integral b_l.

$$b_l(V,T) = \frac{1}{l!\lambda^{3(l-1)}V} \int \left[\sum \prod_{i,j\in\{l\}} f_{ij} \right] dr^{(l)}, \tag{2.4}$$

where the summation goes over all possible products of Mayer's function, that connect the constituents of the cluster. The first order cluster consists of a single

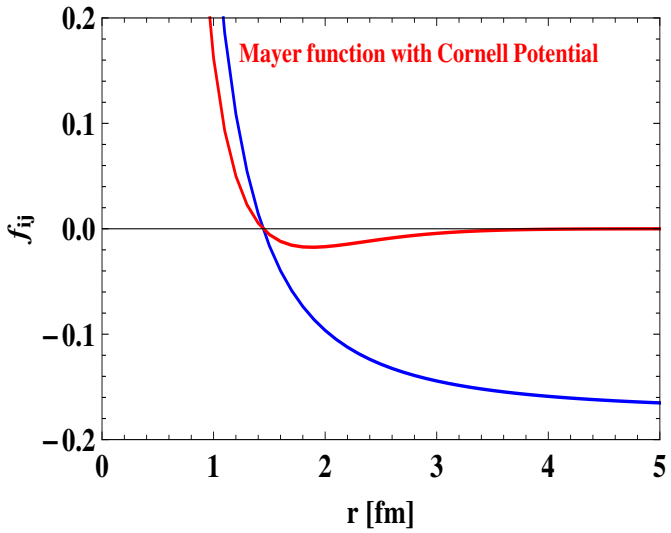

Figure 2.2: Mayer function for Cornell potential (Solid blue line) and Screened Cornell potential (Solid red line).

particle that is not connected with other particles, and the corresponding cluster integral $b_1 = 1$. $b_2 = \frac{1}{2\lambda^3 V} \int f_{ij} dr_i dr_j$ and $b_3 = \frac{1}{6\lambda^6 V} \int (f_{ij}f_{ik} + f_{ij}f_{jk} + f_{ik}f_{jk} + f_{ij}f_{ik}f_{jk}) dr_i dr_j dr_k$ are the second order and third order cluster integrals respectively. Therefore, the configuration integral and hence the partition function can be expressed in terms of the cluster integrals.

After the pioneering work of Mayer in classical systems, Kahn and Uhlenbeck started to develop a mathematical treatment for quantum-mechanical systems. There were inherent difficulties in this analysis, which were removed by Lee and Yang, later by M.V.Ushcats[18, 19].

2.3 Equation of State using Mayer's Cluster Expansion Method

Here, we inspect Mayer's cluster expansion method by taking Canonical partition function of the system [4]. From (2.1) we get,

$$Q_N(V,T) = \sum_{\{m_l\}}{}' \left[\prod_{l=1}^{N} \left(\frac{b_l V}{\lambda^{3l}} \right)^{m_l} \frac{1}{m_l!} \right], \tag{2.5}$$

where λ is the mean thermal wavelength and b_l is the cluster integral. The evaluation of the primed sum in (2.5) is complicated by the restrictive condition

$$\sum_{l=1}^{N} l m_l = N. \tag{2.6}$$

This condition must be obeyed by every set $\{m_l\}$, where $m_l = 0, 1, 2, 3, ..., N$ is the number of clusters. In $Q_N(V,T)$ we take the term with the maximum or equilibrium value of m_l,

$$m_l = \left(\frac{b_l V}{\lambda^{3l}}\right) Z^l, \tag{2.7}$$

where Z is the Lagrange's undetermined multiplier. It is seen from the above equation that the l^{th} term, $\frac{lvb_l}{\lambda^{3l}} Z^l$, of this sum is the fraction of the material in clusters of size l at equilibrium (where $v = \frac{V}{N}$). Substituting equation (2.7) in equation (2.6), we get

$$\sum_{l=1}^{N} \frac{l b_l}{\lambda^{3l}} Z^l = \frac{N}{V} = n. \tag{2.8}$$

Then the equation for $Q_N(V,T)$ is

$$\ln Q_N(V,T) = \sum_{l=1}^{N} \left(\frac{b_l V}{\lambda^{3l}}\right) Z^l - N \ln Z. \tag{2.9}$$

By means of Helmholtz free energy of the system and usual thermodynamic relations, the other thermodynamic properties of the system can be derived. The quantity Z has the dimension of fugacity. If natural system of units is selected the universal constants are normalized to unity. Then the EoS of the system is

$$PV = \{\sum_{l=1}^{N} m_l\} T. \tag{2.10}$$

Hence, the initial non-ideal quark-antiquark plasma has been phase transformed to an ideal system of clusters. A similar equation has been presented within the

frame work of the statistical bootstrap model for an ideal gas [17]. From (2.6) we get $m_1 = N, m_2 = N/2$ and $m_3 = N/3$, as the number of clusters.

From Eq.(2.8), we get the equation of clustering of l quarks and/or anti-quarks with equal mass,

$$n_l = lb_l \left(\frac{MT}{2\pi}\right)^{3l/2} \exp\left(\frac{\mu l}{T}\right), \tag{2.11}$$

where M is the mass of the quarks, μ is the chemical potential and n_l is the number density of the l-particle cluster formed just at the moment, when the clustering takes place. We can write the density of clusters immediately after the phase transition is completed as $n_{quarkcluster} = \frac{n_l}{l}$. We take l=2 for two particle cluster and l=3 for three particle cluster.

Here we take chemical potential μ equal to zero, because after the phase transition the Mesons and Baryons are considered as droplets of quarks and antiquarks, hence no change in the particle number of the quarks and antiquarks takes place.

2.4 Cornell Potential

The well-known Cornell potential also known as the funnel potential [7] is of the form,

$$V = -\frac{\alpha}{r} + \sigma r \tag{2.12}$$

This potential contains the perturbative expectation plus an additional linear term. σ is the string tension, and $\alpha = \frac{4\alpha_s}{3}$, α_s is the strong coupling constant of the color-Coulomb potential. Here the modified Cornell potential is considered,

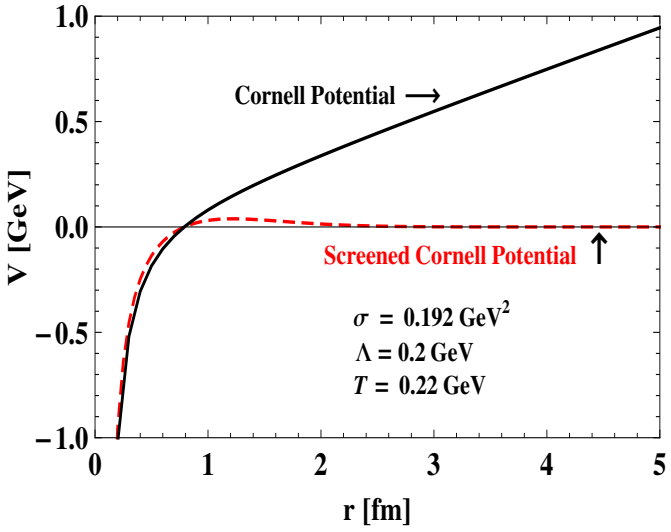

Figure 2.3: Cornell potential and Screened Cornell potential.

$$V = V_Y + V_L \tag{2.13}$$

where V_Y is the screened Coulomb potential (Yukawa potential), V_L is the screened confinement potential [8, 9].

$$V(r,T) = -\frac{\alpha}{r}e^{(-m_D r)} + \frac{\sigma}{m_D}\left[1 - e^{(-m_D r)}\right], \tag{2.14}$$

where $m_D(T) = \left[1 + \frac{N_f}{6}\right]^{1/2} g(T)T$ is the Debye mass and is temperature dependent. When the temperature rises, σ decreases. Above the critical temperature T_c the string breaks and the quarks are deconfined. The Cornell potential and screened Cornell potential are shown in Fig.2.3. We can see that there is a certain duality by defining the heavy quark potential [5]. The term with $\pm\frac{\alpha}{r}$ of the quark potential is the result of gluon exchange between quark-quark or quark-antquark pairs. Thus the potential attain a general form by fixing vertices for particles and antiparticles having reversed signs.

2.5 Equation of State with Screened Cornell Potential

We consider the transition of homogeneous plasma into 2-particle clusters. From Eq.(2.11), the particle density for two quark cluster $l = 2$ at zero chemical potential is,

$$n_{[\text{di-quark cluster}]} = b_2 \left(\frac{M_2 T}{2\pi} \right)^3 . \tag{2.15}$$

The 2-particle cluster integral b_2 is

$$b_2 = \frac{2\pi}{\lambda^3} \int_0^\infty f_{12} d^3 r_{12}. \tag{2.16}$$

Using screened Cornell potential, we get

$$b_2(T) = \frac{2\pi}{3} \left[\frac{1}{m_D^3} + \frac{3}{eT} \left(\frac{5\sigma}{m_D^4} + \frac{2\alpha}{m_D^2} \right) \right]. \tag{2.17}$$

When temperature is increased (above T_c), $m_D(T)$ will increase according to the temperature dependence of the color charge density in statistical QCD and the bounded clusters get deconfined into quark anti-quark sea. In the non-relativistic quark model, the charmonium and bottomonium are described as the $c\bar{c}$ and $b\bar{b}$ bound states.

For the 3-quark clustering ($l = 3$) process, the Eq.(2.11) at μ=0 becomes,

$$n_{[\text{tri-quark cluster}]} = b_3 \left(\frac{M_3 T}{2\pi} \right)^{9/2} . \tag{2.18}$$

The third cluster integral is,

$$b_3 = 2b_2^2 + \frac{1}{6} C_3, \tag{2.19}$$

where

$$C_3 = \int_0^\infty \int_0^\infty f_{12} f_{13} f_{23} d^3 r_{12} d^3 r_{13}. \tag{2.20}$$

We try to numerically evaluate C_3 based on bipolar coordinate integration [6][Appendix-A], by fixing the positions of the particle 1 and 2 whereas particle 3 takes all possible positions. In addition, we use the technique of Jacobian transformation.

$$C_3(T) = 8\pi^2 \int_{r=0}^\infty r_{12}^2 f(r_{12}) \int_{r=0}^\infty r_{13}^2 f(r_{13}) \int_{r=-1}^1 f(\sqrt{r_{12}^2 + r_{13}^2 - 2r_{12}r_{13}\mu}) d\mu dr_{12} dr_{13}, \tag{2.21}$$

Where $\mu = \cos(\theta)$, θ is the angle between r_{12} and r_{13}.

The generalised EoS for the cluster system, containing different quarks having different mass is obtained from Eq.(2.11) is of the form,

$$n_l = l b_l \prod_{i=1}^{l} \left(\frac{M_i T_i}{2\pi} \right)^{(3l)/2},$$

where M_i and T_i are the mass and critical temperature respectively.

2.6 Results and Discussion

Mayer cluster expansion method in the case of deconfined matter have been analysed. Based on this model we have examined the properties of a thermalized quark-antiquark plasma and investigated the dissociation of heavier hadrons in QGP. The main advantage of the above mentioned method is that we can apply the classical particle picture to the quarks and investigate clustering of quarks in a QGP.

We have obtained EoS that relate particle number density (n) at various temperatures (T) for the quarkonium states, such as J/ψ meson (charmonium $c\bar{c}$) (Fig.2.4) and Υ meson (bottomonium $b\bar{b}$) (Fig.2.5). We have observed a sudden

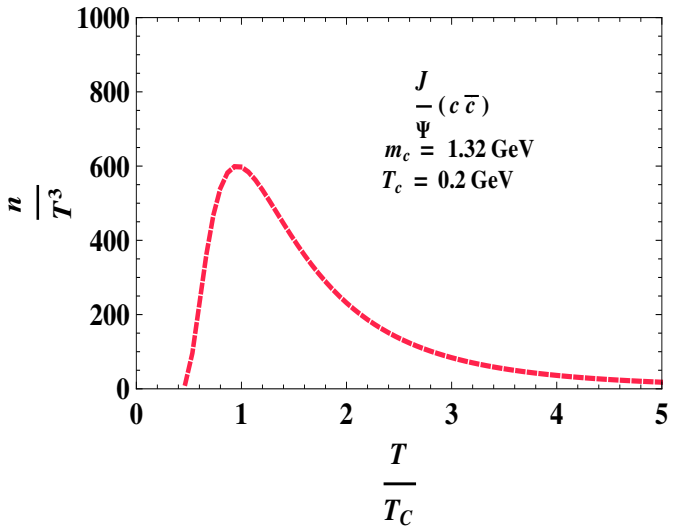

Figure 2.4: Plot of n as a function of T for the dissociation of charmonium in QGP ($c\bar{c} \longleftrightarrow J/\Psi$).

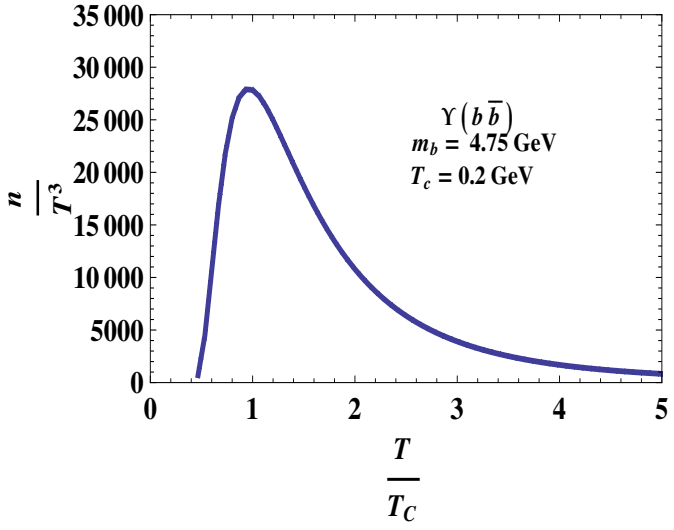

Figure 2.5: Plot of n as a function of T for the dissociation of bottomonium in QGP ($b\bar{b} \longleftrightarrow \Upsilon$).

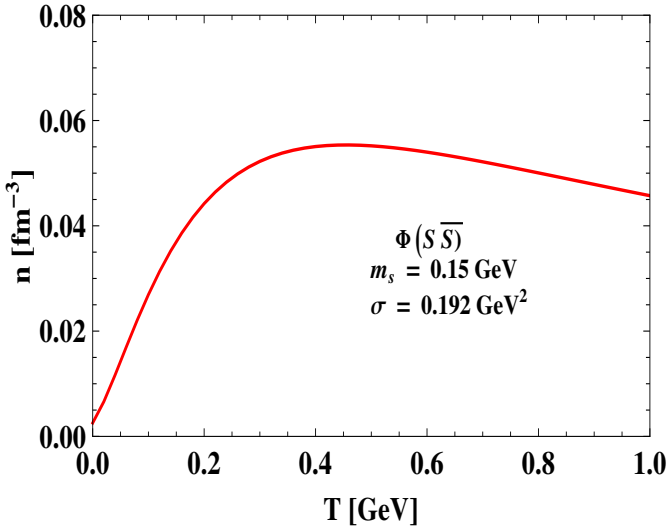

Figure 2.6: Plot of number density (n) as a function of temperature T using Cornell potential for the clustering of two strange quarks in QGP.

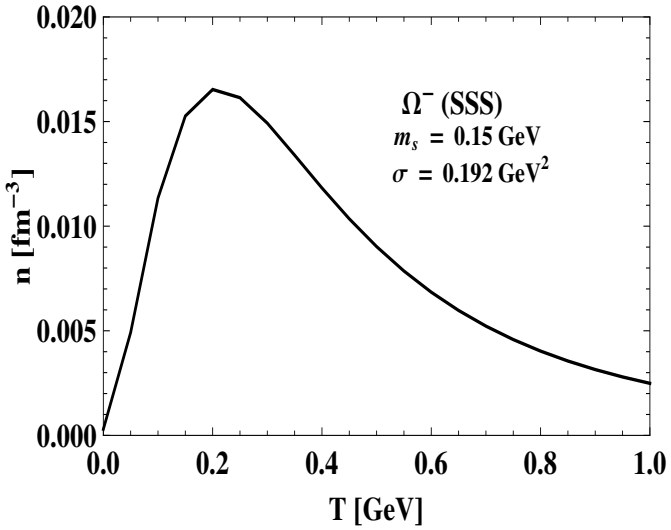

Figure 2.7: Plot of n as a function of T using Cornell potential for the clustering of three strange quarks in QGP.

Table 2.1: Multi-Strange Hadronization using Screened Cornell Potential

Quarks	$s\bar{s}$	sss	ssc	scc	$c\bar{s}$	$ss\bar{b}$
Symbol	ϕ	Ω^-	Ω_c^0	Ω_{cc}^+	D_s^+	Ω_b^-
$n[fm^{-3}]$	2.10^{-2}	3.10^{-3}	1.10^{-1}	2	5.10^{-1}	5

peak at the heavy quark clustering region, i.e, near the transition temperature. The statistical bootstrap model observed a pronounced maximum for the number density close to the critical temperature. Theoretical results and Lattice calculations show the existence of heavy bound state above T_c, up to $2.5T_c$

Fig.2.6 and Fig.2.7 shows the enhancement of strange droplets near the transition temperature T_c. Here we have plotted the number density of $\Phi(s\bar{s})$ meson and $\Omega^-(sss)$ baryon system for various temperature range. The number density of the different strange particle near the transition region,T_c are tabulated in Table: 2.1.

Bibliography

[1] T. Matsui and H. Satz, Phys. Lett. B 178, 416 (1986).

[2] M. C. Abreu et al., Phys. Lett. B 477, 28 (2000).

[3] J. E. Mayer and M. G. Mayer, Statistical Mechanics, Wiley, Chaps.13 and 14 (1946).

[4] R. K. Pathria, Statistical Mechanics, Pergamon Oxford, Chaps.9 and 12 (1972).

[5] Bijan Sheikholeslami-Sabzevari, Phys. Rev. C 65, 054904 (2002).

[6] Artit Hutem, Sutee Boonchui, J. Math. Chem. 50 ,1262-1276 (2012).

[7] F. Karsch, M. T. Mehr, and H. Satz, Z. Phys. C 37, 617 (1988).

[8] M Doring, K Hubner, O Kaczmarek, F Karsch Phys. Rev D 75, 054504 (2007).

[9] Jiao-Kai Chen, Phys. Rev. D 86, 036013 (2012).

[10] Helmut Satz, Nuclear Physics A 783, 249 (2007.

[11] Edward V. Shuryak and Ismail Zahed, Phys. Rev. D 70, 054507 (2004).

[12] J. Rafelski, Phys. Rep. 88, 331 (1982).

[13] WA97 Collaboration, E. Andersen et al., Phys. Lett. B 449, 401 (1999).

[14] V. M. Bannur, Phys. Lett. B 362, 7-10 (1995).

[15] K. M. Udayanandan, P. Sethumadhavan, and V. M. Bannur, Phys.Rev.C 76, 044908 (2007).

[16] R. Hagedorn and J. Rafelski, Phys. Lett. B 97, 136 (1980).

[17] R Hagedorn, J Rafelski, Statistical Mechanics of Quarks and Hadrons, pp 237-249 (1981).

[18] M.V. Ushcats, PRL 109, 040601 (2012).

[19] M. V. Ushcats, J. Chem. Phys. 138, 094309 (2013).

Chapter 3

Phase Transition Studies in Quark-Gluon Plasma

3.1 Introduction

The study of the fundamental theory of strong interactions, QCD, under extreme conditions of temperature and density has been one of the most challenging problems in physics. A primary goal of relativistic nuclear collisions is the observation of a phase transition of confined, hadronic matter to a deconfined quark-gluon plasma [1, 2]. The phase transition plays a significant role in statistical mechanics as well as other fields including QFT at finite temperature.

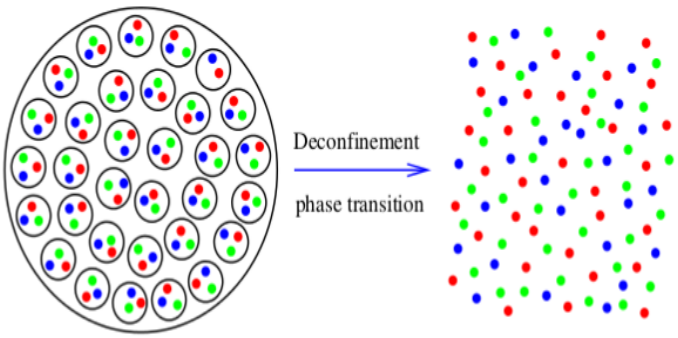

Figure 3.1: Transition from Confined state to deconfined state.

The most important approach to derive the Virial Equation of State (VEoS) was given by Mayer [3, 4] and his collaborators. Using cluster expansion method, Mayer was able to express the partition function as a series of expansion in powers of density. The first limitation of this method is that the density should be small so as to satisfy the convergence condition. In addition to this there exists a strong limitation that restricts density more strictly, given by,

$$\sum_{k\geq 1} k\beta_k \rho^k < 1. \tag{3.1}$$

This limitation on density is related to the radius of convergence and makes it impossible to predict the region of condensation. So, the phenomena of phase transition cannot be proved using classical statistical mechanics. Ushcats, using analytical complex calculation, [5, 6] have shows that, it is possible to neglect the forbidden region in Mayer's equation of state, where the equation of state cannot be defined. The equation, as derived by Ushcats, clearly demonstrates the process of condensation at high density region. A modified generating function for the canonical partition function has been derived [7]. Using this generating function, the author analysed again Mayer's theory of classical cluster expansion and studied Mayer's theory of virial expansion and condensation at thermodynamic limit.

The main purpose of this work is to produce an equation of state for QGP, using the mathematical formalism of Ushcats [6]. Here, we use the interacting potential as modified Cornell potential [9], in which the Cornell potential [11, 12] is modified by including a screening effect. Earlier calculation of EoS for QCD phase transition mainly focused on finite temperature and zero chemical potential, but here we inspect the phase transition using modified version Mayer's condensation method which is extended in high density regime. The volume is varied keeping temperature fixed and the corresponding pressure is calculated. The same can be done by changing the density ρ, as done by Ushcats [5, 6] using the Lennard-Jones potential.

3.2 EoS in terms of Irreducible Cluster Integrals

Mayer improved the Cluster expansion method by restructuring the cluster integrals. They introduced the irreducible cluster integral as one that cannot be further reduced into products. The second order cluster integral b_2 cannot be split to simpler integrals and should be considered as the first order irreducible cluster integral β_1 as,

$$b_2 = \frac{1}{2}\int_{r_{ij}} f_{ij} dr_{ij} = \frac{1}{2}\beta_1,$$

where

$$\beta_1 = \int_{\infty} f_{ij} dr_{ij}.$$

Here integration over the real phase-space of the j^{th} particle relative to the position of the i^{th} particle is replaced by the integration over infinite volume. Similarly the third order cluster integral can express in terms of first order and second order irreducible cluster integral as given below,

$$b_3 = \frac{1}{2}\beta_1^2 + \frac{1}{3}\beta_2,$$

where,

$$\beta_2 = \frac{1}{2!}\int_{\infty} f_{ij} f_{ik} f_{jk} dr_{ij} dr_{ik}.$$

Generally, the cluster integral b_l can be expressed as a sum of terms with irreducible cluster integral β_k's.

$$b_l = \frac{1}{l^2}\sum_{\{n_k\}}{}' \prod_k \frac{(l\beta_k)^{n_k}}{n_k!} \tag{3.2}$$

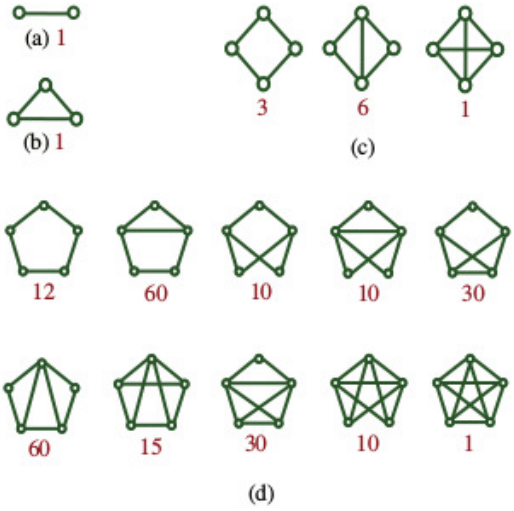

Figure 3.2: Irreducible two, three, four and particle graphs. The number represents the multiplicity of a graph.

where the restricted summation goes over all the sets $\{n_k\}$ with the condition

$$\sum_k k n_k = l - 1 \tag{3.3}$$

The diagrammatic representation of β_k's are expressed in Fig.3.2. The virial coefficient B_{k+1}'s are related to the corresponding irreducible cluster integral β_k's.

$$B_{k+1} = -\frac{k}{k+1}\beta_k.$$

Using complex combinatorial methods, Mayer derived the Virial expansion for pressure. The maximum term in Q_N is found and equating to logarithm of density and activity results in,

$$ln\Big(\frac{Q_N}{N!}\Big) = N\Big[1 + \sum_{k\geq 1}\frac{1}{k+1}\beta_k\rho^k + ln(\rho)\Big]. \tag{3.4}$$

From the above relation the thermodynamic properties of the imperfect gas can be derived. The equation of state (EoS) obtained from the above relation has

the form,

$$\frac{PV}{Nk_BT} = 1 - \sum_{k\geq 1} \frac{k}{k+1}\beta_k \rho^k, \tag{3.5}$$

Here all irreducible integrals are replaced by finite one. In fact, the β_l of the same order belonging to various b_l must differ, but, due to the simplification they become identical. This simplification is adequate only for low density region. For high density regime, the irreducible cluster integrals β_k may considerably differ from the similar cluster integrals b_l and this issue is specially discussed by Ushcats [5, 6].

The first limitation of Mayer's method is that the density ρ should be small, which signifies the convergence condition. There exists a volume ν_f below which the b_l's are volume independent. This volume corresponds to the volume of the condensed phase. Another critical volume denoted as ν_s called volume of the saturated vapour exists [3] for which $\left(\frac{\partial P}{\partial V}\right)_T = 0$. Between these two critical volumes the system undergoes a change of phase known as condensation.

Differentiating the equation of state Eq.3.5 with respect to the volume V and at $\left(\frac{\partial P}{\partial V}\right)_T = 0$, there exists a density $\rho_s = \frac{1}{\nu_s}$, where the value of ρ_s is obtained as the positive roots of the equation,

$$\sum_{k\geq 1} k\beta_k \rho_s^k = 1,$$

where ρ_s is the critical density at which the system undergoes a change of phase. This leads to another restriction of Mayer's method, which limits the density more strictly.

$$\sum_{k\geq 1} k\beta_k \rho^k < 1,$$

A critical temperature T_c exists, above which there is no condensation range. A second characteristic temperature T_m exists which is lower than T_c. At the critical temperature T_c, $\sum k\beta_k\rho^k = 1$ and $(\frac{\partial P}{\partial V}) = 0$. Below the critical temper-

ature T_c, the maximum value of $\sum k\beta_k\rho^k > 1$ and the roots are positive. At temperature above the critical temperature $T_c, \sum k\beta_k\rho^k < 1$ and $(\frac{\partial P}{\partial V})$ is negative at all volumes. The phenomena associated with condensation appears only below T_m. In this region $\sum k\beta_k\rho^k < 1$, which is one of the strong limitations in Mayer's theory of condensation.

3.3 High Density EoS and the Theory of Condensation.

Ushcats made an EoS for the finite number of particles that showed significant differences in comparison with the virial expansion at high densities [5]. The key element of this approach is the exact generating function for the partition function in the form of Mayer's cluster expansion. The configuration integral (Z_N) obtained by Mayer is the coefficient in the power series expansion of density and fugacity. Using a quite similar approach it is possible to express the partition function $(Q_N/V^N N!)$ as the coefficient at y^N in the power expansion of the function given by,

$$F(y) = \left(1 - \sum_{k\geq 1} k\beta_k y^k\right) \exp\left(N\left[\frac{y}{\rho}\left(1 - \sum_{k\geq 1}\frac{k}{k+1}\beta_k y^k\right) + \sum_{k\geq 1}\beta_k y^k\right]\right).$$

The N^{th} coefficient in the Taylor series expansion of this function gives the configuration integral,

$$Z_N = V^N q_N,$$

where

$$q_N = \Big(\frac{\partial^N F(y)}{\partial y^N}\Big)_{y=0}.$$

Evaluating q_N we get,

$$q_N = M_N - \sum_{k=1}^{N} \frac{N!}{(N-k)!} k \frac{\beta_k \rho^k}{N^k} M_{N-k}. \tag{3.6}$$

Here the values of M_k are defined by the recurance relation,

$$M_k = M_{k-1} + \sum_{i=1}^{k} \frac{i\beta_i \rho^i}{N^{i-1}} \frac{(k-1)!}{(k-i)!} \Big[M_{k-i} - \frac{(k-i)}{N} M_{k-1-i} \Big], \tag{3.7}$$

with $M_0 = 1$ and $M_{k<0} = 0$.

The free energy can be calculated after knowing the partition function of system using the relation, $A = -k_B T ln(Q_N)$. We can derive the Cluster expansion EoS for finite size system (fEoS) using the relation, $P = -\frac{\partial A}{\partial V}$, as,

$$\frac{P}{T} = \frac{q_{N-1} - \sum_{k=1}^{N-1} \frac{k}{k+1} \beta_k q_{N-k-1}}{q_N}. \tag{3.8}$$

The relation Eq.(3.5) is the simplification of Eq.(3.8) in the thermodynamic limit and $\frac{(N-1)!}{(N-1-k)!} \to N^k$.

For large N values, i e., system with large number of particles, the density $\rho \geq \rho_0$, where ρ_0 is the minimum density that violates the condition,

$$\sum_{k \geq 1} k \beta_k \rho_0^k = 1. \tag{3.9}$$

We want to eliminate the dependence on N from Eq.(3.8) at the thermodynamic limit and reconstruct an equation of state that is valid at very small and very large values simultaneously. The recursive relation in the Taylor series represented by M_k can be considered as a function of $Z(\rho)$, where it is defined as the ratio given by

$$Z_k = \frac{M_k}{M_{k-1}} = 1 + \sum_{i=1}^{k} \frac{i\beta_i \rho^i}{N^{i-1}} \frac{(k-1)!}{(k-i)!} \Big[\frac{M_{k-i}}{M_{k-1}} - \frac{(k-i)}{N} \frac{M_{k-1-i}}{M_{k-1}} \Big].$$

For large value of N, we can assume that $Z_{N-1} \approx Z_N \approx Z$. The above equation

can be rewritten as,

$$Z = 1 + (Z-1)\sum_{k\geq 1} \frac{k\beta_k \rho^k}{Z^k}.$$

Clearly one of the roots of the equation is $Z = 1$, and the other roots are given by the relation

$$\sum_{k\geq 1} k\beta_k \Big(\frac{\rho}{Z}\Big)^k = 1. \tag{3.10}$$

Thus the EoS in Eq.(3.8) can be written in terms of Z as,

$$\frac{PV}{Nk_BT} = \frac{1 - \sum_{k\geq 1} \frac{k}{k+1}\beta_k (\frac{\rho}{Z})^k}{Z}. \tag{3.11}$$

At the temperature below the critical temperature the irreducible cluster integrals at low density are such that, they satisfy the condition Eq.(3.10) and $Z = 1$. At higher density $\rho > \rho_0$ the condition is violated. In this region the M_k values are such that it forms an increasing pattern and $Z > 1$. So the range of values for Z can be defined as,

$$Z(\rho) = \begin{cases} 1; & \rho \leq \rho_0 \\ \frac{\rho}{\rho_0}; & \rho > \rho_0. \end{cases} \tag{3.12}$$

Applying Eq.(3.12) in Eq.(3.11), the cluster expansion EoS (CEEoS) acquires the following piecewise form in the thermodynamic limit,

$$\frac{P}{k_BT} = \begin{cases} \rho\Big(1 - \sum_{k\geq 1} \frac{k}{k+1}\beta_k \rho^k\Big); & \rho \leq \rho_0 \\ \\ \rho_0\Big(1 - \sum_{k\geq 1} \frac{k}{k+1}\beta_k \rho_0^k\Big); & \rho > \rho_0. \end{cases} \tag{3.13}$$

where ρ_0 is the minimum real positive root of Eq.(3.9). At high density region, $\rho > \rho_0$, the above equation (Eq.3.13) is valid and gives a clear description of con-

densation. For a system of interacting particles, this EoS has provided the strong analytical relation instead of the conventional activity series, which diverges at high-density regimes. The inherent limitation of the present EoS is that, beyond the condensation point, the CEEOS pressure stays constant even at $\rho \to \infty$.

3.4 Condensation in Modified Cornell Potential

The Cornell potential model has been used earlier to obtain the EoS and compared with the lattice QCD results of the QGP [10, 11]. Sheikholeslami-Sabzevari [12] had obtained an EoS for hot QGP transition to hadrons with full QCD potential analytically. In this work we obtain the exact EoS for QGP using the modified Cornell potential which is also valid in high density regime. In order to study the statistical mechanics of phase transition in modified Cornell potential, the first step is to evaluate the irreducible cluster integrals.

Here the system consists of sea of quarks, which condenses into two particle and three particle clusters having irreducible cluster integral β_1 and β_2 respectively. One of the main difficulties is the calculation of irreducible cluster integral. For small k values i.e., up to $k = 2$, we can easily calculate the value of β_k. The first irreducible cluster integral β_1 is calculated using the relation,

$$\beta_1 = \frac{-4\pi}{\lambda^3} \int_0^\infty \Big[1 - \exp\Big(\frac{-U(r)}{k_B T}\Big)\Big] r^2 dr. \tag{3.14}$$

where λ is the thermal wavelength and $U(r)$, the interacting potential.

The second order irreducible cluster integral has been approximately evaluated in [8]. The same method is adopted for numerically evaluating the second order irreducible cluster integral β_2.

Here the interaction potential is modified Cornell potential [9, 12], which is given by,

$$U(T) = \sigma r_D (1 - e^{-\frac{r}{r_D}}) - \frac{\alpha_s}{r} e^{-\frac{r}{r_D}}. \tag{3.15}$$

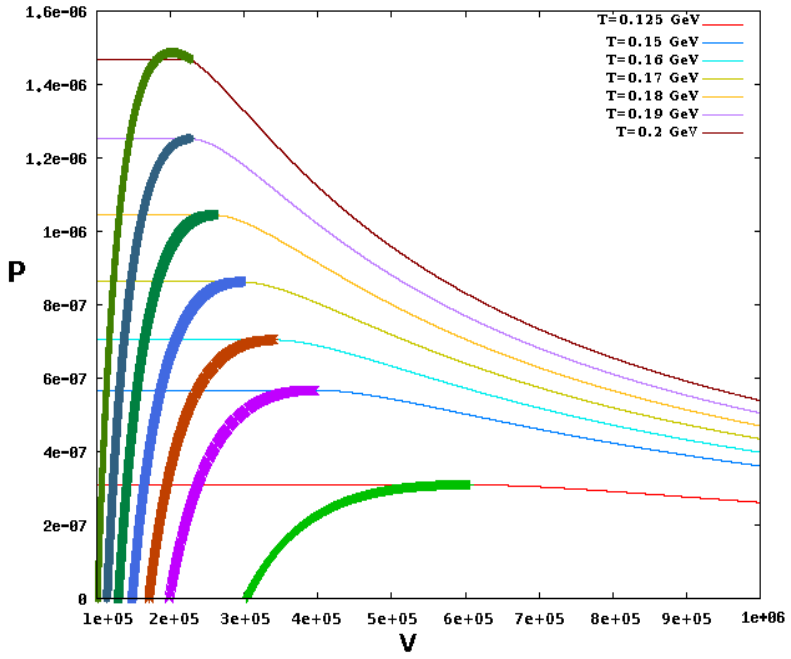

Figure 3.3: Isotherm for different temperatures using modified Cornell potential. V in GeV^{-3} and P in GeV^4.

We consider a system with Charm quarks having the following parameters. The running coupling constant $\alpha_s = 0.471$ and $\sigma = 0.192\ GeV^2$. The Debye screening length $r_D = 2.13\ GeV^{-1}$ (Inverse of the screening mass m_D) with the bare mass of about $1.32\ GeV$.

To calculate the EoS Eq.(3.8), one need to solve q_1, q_2, q_3, M_1, M_2 and M_3 [See appendix -B]. Knowing the values of β_1 and β_2, using the equation of state and Virial equation of state is calculated by varying volume. From the numerically plotted isotherm, we can see the variation of pressure for different number of particles. The point at which the equations of state corresponding to lower and higher density (total density of charm quarks) regions coincide is the point ρ_0 where the condition is violated. This can easily be understood from the Eq.(3.13). So we can establish the equation of state where the Virial expansion is not applicable. The behaviour of these equations specifies the phase transition. The constant pressure indicates that, the point where the curves meet corresponds to the saturated vapour density.

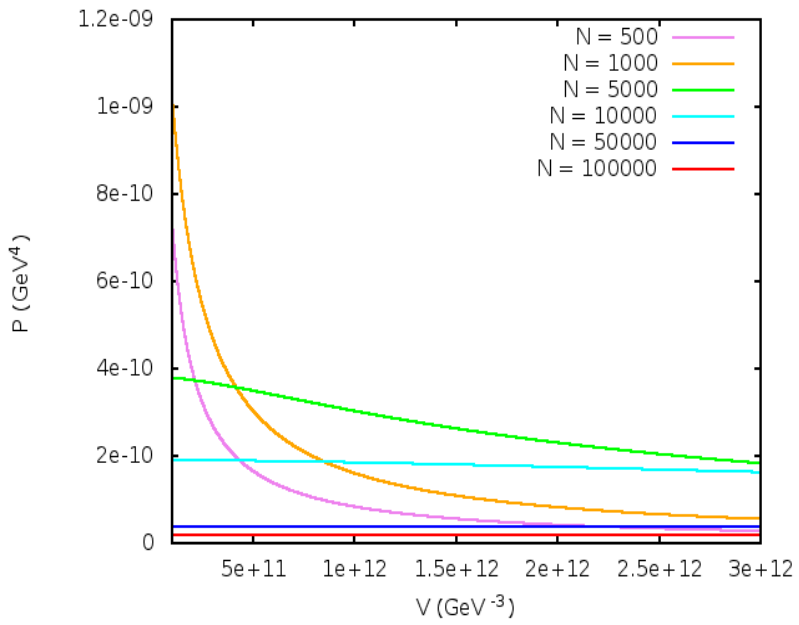

Figure 3.4: Isotherms for temperature T = 0.17 GeV, for modified Cornell potential for the volume, ranging from $1 \times 10^{11} \rightarrow 3 \times 10^{12}\ GeV^{-3}$.

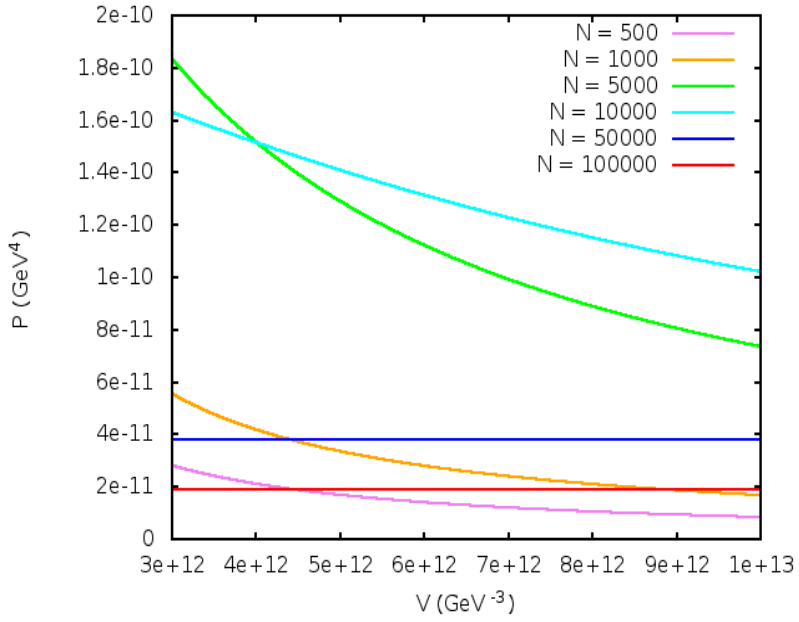

Figure 3.5: Isotherms for temperature T = 0.17 GeV, for modified Cornell potential for the volume, ranging from $3 \times 10^{12} \rightarrow 1 \times 10^{13}\ GeV^{-3}$.

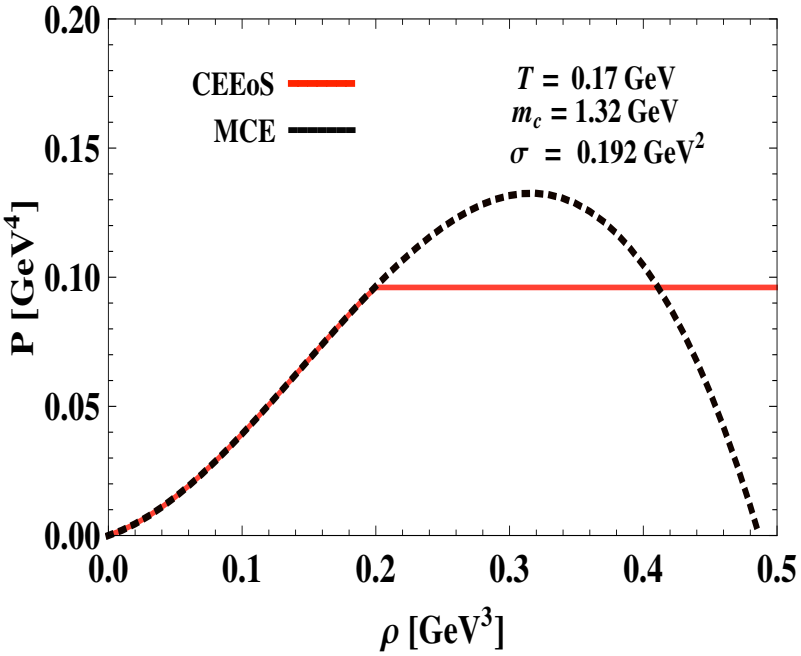

Figure 3.6: A comparison of the Mayer's relation and Ushcats relation for modified Cornell potential, T = 0.17GeV.

3.5 Results and Discussion

Using the classical statistical method of condensation by Mayer, which was modified by Ushcats, an equation of state is derived which is applicable to the region where it was forbidden. Using this method, it is possible to find the region of condensation for QGP. A satisfactory result is obtained for the modified Cornell potential, which is in agreement with other theoretical results.

Fig. 3.3 gives the EoS for different temperature range for the modified Cornell Potential. The critical point where the system converge will be different for different temperature. As the temperature increases, the system will evolve to the QGP state. This region is shown in the figure (temperature is within 0.16 GeV - 0.19 GeV), which clearly express the critical point of phase transition. Similar argument were proposed by Lattice QCD.

Fig. 3.4 and Fig. 3.5 gives the equation of state for different number of quarks. As the number of particles increases, the region where the system condenses changes, so that the critical point will be different for different number of

particles. When the number of particle N increases, this high density interval of isotherms becomes more flat. The region of convergence can be understood for different number of particles. The same system in a different range of volume have a quite similar result.

Using the Ushcats method of cluster expansion, it is possible to explain the phenomena of phase transition and the region of condensation. A comparison of the two numerical results obtained using Mayer's relation Eq.(3.5) and Ushcats relation Eq.(3.13) is made for modified Cornell potential, and is plotted in Fig. 3.6 at various densities. We can see that, the two curves clearly get crossed over one another after a particular value of density and the CEEoS Eq.(3.13) is valid in all density region.

Bibliography

[1] M. Cheng et al., Phys. Rev. D 77, 014511 (2008).

[2] Y. Aoki, Z. Fodor, S.D. Katz et al., Phys. Lett. B 643, 46 (2006).

[3] J.E Mayer and M.G. Mayer, Statistical Mechanics (Wiley New York, 1977).

[4] R.K. Pathria, Pergamon International Library of Science, Engineering, Technology and Social studies, 1972.

[5] M.V. Ushcats, PRL 109, 040601 (2012).

[6] M. V. Ushcats, J. Chem. Phys. 138, 094309 (2013).

[7] Vishnu M. Bannur, Physica A 419, 675–680 (2015).

[8] Artit Hutem, Sutee Boonchui, J Math Chem 50, 1262–1276 (2012).

[9] Matthias Doring, Kay Hubner, Olaf Kaczmarek, and Frithjof Karsch, Phys. Rev. D 75, 054504 (2007)

[10] V. M. Bannur, Phys. Lett. B362, 7 (1995).

[11] K. M. Udayanandan, P. Sethumadhavan, and V. M. Bannur, Phys. Rev. C 76, 044908 (2007).

[12] B. Sheikholeslami-Sabzevari, Phys. Rev. C 65, 054904 (2002).

Chapter 4

Transport Coefficients of Quark-Gluon Plasma

4.1 Introduction

The experimental findings of RHIC at the BNL [1] and ALICE detector at the CERN Large Hadron Collider [2], confirm the 'almost perfect fluidity' of the strongly coupled quark-gluon plasma. The analysis of elliptic flow based on viscous hydrodynamic model showed that, the QGP has a very small value of specific viscosity η/s 0.08 - 0.24 [4, 5, 6, 7], quite close to the conjectured lower-bound limit $\eta/s \geq 1/(4\pi)$ within the anti-de Sitter/conformal field theory (AdS/CFT) correspondence [8, 9]. This suggests that, hot QCD matter could be a nearly perfect fluid, i.e, η/s reaches a minimum at near the critical temperature and increases thereafter in the deconfined phase [10, 11]. The lattice calculations [11, 12, 13] of QCD plasma do support the current estimates.

The role of bulk viscosity of QGP has achieved considerable attention in the late stage of relativistic heavy-ion collisions. The bulk viscosity in the context of the violation of scale invariance in QCD [16, 17] is reported. It was found that the bulk viscous coefficient ζ has a prominent peak around the critical region. The effect of bulk viscosity in freeze-out [18, 19] and in hadronic phase have been reported in [20]. Several calculations of the bulk viscosity in the context of cosmology [21], strange quark matter [22], and neutron stars [23] have been performed.

We focus on the effects of shear viscosity and bulk viscosity in the relativistic heavy-ion collisions, in particular near the transition region. Earlier calculations of the ratio of shear viscosity to the entropy density η/s in the deconfined phase

were done in [25]. Mattiello et al., calculated the QCD equation of state using the virial expansion approach [26]. For an application of this formalism to QGP, the interaction between quarks has to include nonperturbative effects from dimension two gluon condensates that describe the free energy of quenched QCD. Instead of virial series expansion, we consider cluster expansion method [23, 24]. Mayer's theory of plasma described by Balescu [29] is used to derive a compact expression for the equation of state of QGP. We use modified Cornell potential [36, 37] to take into account the interaction between partons in QGP.

An imperfection of Mayer's cluster expansion method [23] is that the density should be small so as to satisfy the convergence condition. An equation is derived by Ushcats [30, 31] which establish the process of condensation in high density regions and find an equation of state (EoS) for real gas using the Lennard-Jones potential. QGP phase transition was studied and an EoS derived using the same in [32], where a satisfactory result was obtained for the phase transition and region of condensation of QGP with the modified Cornell potential. A modified generating function for the canonical partition function has been derived [33]. Using this generating function, the author studied the Mayer's theory of virial expansion and condensation at thermodynamic limit. Mayer's theory of plasma is described in [29], where one sums a certain set of infinite diagrams. Going beyond, a generalization of the cluster expansion method was developed in [25, 35] to calculate the QCD equation of state. Here we use the cluster expansion method to take into account and present a detailed derivation of the equation of state and hence the entropy density of the QGP at vanishing μ_q. Instead of phenomenological models like quasi-particle models [4, 5], the cluster integral in the cluster expansion method includes the interaction potential between the partons. The interaction between the partons is described by modified Cornell potential [36, 37] which incorporates the screened color-Coulomb potential and the screened linear potential [38].

To calculate the transport coefficients, we use the relativistic extension of the Chapman-Enskog method [43, 44]. The Chapman-Enskog approximation features the transport cross section and hence the interaction. A quantitative comparison between the results of shear viscosities from the Chapman-Enskog and relaxation time methods for selected test cases is performed [45]. This leads to the calculation of transport coefficients in the case of the QGP. From the modified Cornell potential, we have directly extracted the effective coupling α_V to be employed for the determination of the transport cross section which enters

the transport coefficients η and ζ.

4.2 EoS using Cluster Expansion Theory of Plasma

Mayer's theory of plasma is described in [29]. The pressure is given by,

$$\frac{P}{T} = \sum_{i=1}^{N} n_i + D - \sum_{i\geq 1}^{N} n_i \frac{\partial D}{\partial n_i} \tag{4.1}$$

in natural units. For gluons let the number density n_i be represented by n_g, for quarks and the antiquarks n_q, $n_{\bar{q}}$ respectively. D is the sum over all clusters.

$$D = \frac{1}{4\pi^2} \int_0^\infty l^2 dl \left[\frac{(-\kappa^2 V_l)^2}{2} + \frac{(-\kappa^2 V_l)^3}{3} + ... \right] \tag{4.2}$$

The inverse Debye length squared varies as,

$$\kappa^2 = \frac{n_g}{T}, \tag{4.3}$$

for gluon plasma and

$$\kappa^2 = \frac{n_q + n_{\bar{q}}}{T}, \tag{4.4}$$

for quark-antiquark plasma.

Thus the EoS (4.1) for gluon plasma and quark-antiquark plasma has the same appearance with different values for κ^2,

$$\frac{P}{T} = \kappa^2 T + D - \kappa^2 \frac{\partial D}{\partial \kappa^2}. \tag{4.5}$$

For gluon plasma,

$$n_g \approx \frac{g_I}{\pi^2} T^3 \sum_{l=1}^{\infty} \frac{1}{l^3} = g_I T^3 \frac{\zeta(3)}{\pi^2}, \tag{4.6}$$

where g_I=16 is the internal degrees of freedom for gluons and $\zeta(3)$=1.202 is the Riemann-zeta function.

For quark-antiquark plasma,

$$n_q + n_{\bar{q}} \approx \frac{12 n_f}{\pi^2} T^3 \sum_{l=1}^{\infty} \frac{(-1)^{l-1}}{l^3} = \frac{12 n_f}{\pi^2} T^3 \frac{3}{4} \zeta(3). \tag{4.7}$$

Where n_f is the number of flavours of the quark anti-quark plasma.

Taking Eq.(4.2) and differentiating with respect to κ^2, we get,

$$\frac{\partial D}{\partial \kappa^2} = \frac{\kappa^2}{4\pi^2} \int_0^{\infty} l^2 dl \frac{\kappa^2 V_l}{1 + \kappa^2 V_l}, \tag{4.8}$$

where V_l is the interaction potential in momentum space.

Here the interaction potential between the constituents described by modified Cornell potential,

$$\grave{V}(r_{ij}) = \left(\frac{\alpha}{r_{ij}} - \sigma r_{ij} \right) \exp\left(-m_D r_{ij}\right) \tag{4.9}$$

contains the coulomb plus an additional linear term. The contribution of screening effect is coming via the exponential term in the potential. $\alpha = \frac{4\alpha_s}{3}$ for quark-antiquark plasma and $\alpha = 3\alpha_s$ for gluon plasma, where α_s is the strong coupling constant of the color Coulomb potential and σ is the string tension. The Casimir scaling ($C = 9/4$) has been included in the potential of gluon plasma for obtaining an exact EoS of QGP [39, 40]. The interaction potential in plasma is generally defined as, $V(r,T) = z_i z_j \acute{V}(r_{ij})$, where $z_i = 1$ or $z_i = -1$ if the particle is quark or antiquark respectively. The Cornell potential does not depend on the nature of the particles. By taking Fourier transform of modified Cornell potential Eq.(4.9), we get

$$V_l = \frac{16\pi\alpha_s}{3(m_D^2 + l^2)} + \frac{8\pi\sigma}{(m_D^2 + l^2)^2} - \frac{32\pi m_D^2}{(m_D^2 + l^2)^3}. \tag{4.10}$$

where $m_D(T) = \left[1 + \frac{N_f}{6}\right]^{1/2} g(T) T$ is the Debye mass.

Substituting Eq.(4.10) in Eq.(4.8) and integrating over l gives $\frac{\partial D}{\partial \kappa^2}$. D is obtained by integrating over κ^2. Substituting the above in Eq.(4.5), gives the pressure as function of temperature. By substituting Eq.(4.3) and Eq.(4.4) in Eq.(4.5) gives the equation of state of state of quark-anti quark plasma and gluon plasma respectively. We obtain the QGP equation of state by adding these separate contributions,

$$\frac{P}{T^4} = \frac{P_{q\bar{q}}}{T^4} + \frac{P_g}{T^4}. \tag{4.11}$$

The other thermodynamic quantities can be calculated from the pressure P using thermodynamic relations, in particular, the entropy density, $s(T) = \frac{\partial P}{\partial T}$. The pressure $P(T)$ and total entropy density $s(T)$ of QGP are plotted in Fig.4.1 and Fig 4.2 respectively.

4.3 Transport Coefficients of QGP

The general expression for the transport coefficient like shear viscosity η, bulk viscosity ζ are taken from the Chapman-Enskog approximation [45].

$$\eta = \frac{T\psi^2}{10a} \tag{4.12}$$

$$\zeta = \frac{T\phi^2}{b}, \tag{4.13}$$

where ψ and ϕ are temperature dependent and interaction independent functions respectively.

$$\psi = -10\frac{K_3(z)}{K_2(z)}, \tag{4.14}$$

$$\phi = \frac{3}{2}\left(zh\left(\frac{C_p}{C_v} - \frac{5}{3}\right) + \frac{C_p}{C_v}\right), \tag{4.15}$$

where $K_2(z)$, $K_3(z)$ are the modified Bessel function of the second kind of order two and three respectively. It depends on a dimensionless quantity $z = \frac{m}{T}$, where m is the particle mass and T is the temperature.

The parameters a and b in Eq.(4.12) and Eq.(4.13) are combinations of integrals depending on the particle interaction,

$$a = 16\left(\omega_2^{(2)} - z^{-1}\omega_1^{(2)} + \frac{1}{3}z^{-2}\omega_0^{(2)}\right), \tag{4.16}$$

$$b = 2\omega_0^{(2)}, \tag{4.17}$$

Here omega function is defined as,

$$\omega_i^{(s)}(z) = \frac{2\pi z^3}{K_2^2(z)} \int_0^\infty \sinh^7(u)\cosh^i(u)K_j$$
$$(2\mathrm{zcosh}(u)du \int_0^\infty \sin\theta \frac{d\sigma(u,\theta)}{d\Omega}(1-\cos^s\theta)d\theta \quad (4.18)$$

where $j = \frac{5}{2} + \frac{1}{2}(-1)^i$. The particle interaction is encoded in the differential cross section $\frac{d\sigma(u,\theta)}{d\Omega}$. The integration variable u is connected to the relative momentum $p = m\sinh u$ and total momentum $P = 2m\cosh u$ of the two colliding particles and θ denotes the scattering angle in the center of momentum frame. Performing integration by putting $x = \cosh u$ in Eq.(4.18) and connecting with transport cross section $\sigma_t = \int \frac{d\sigma}{d\Omega}\sin^2\theta d\Omega$, we get,

$$\omega_i^{(2)}(z) = \frac{\sigma_t z^3}{K_2^2(z)} \int_1^\infty (x^2-1)^3 x^i K_j(2zx)dx \quad (4.19)$$

Using Eq.(4.14)-Eq.(4.19) and the Bessel function $K_2(z)$ and $K_3(z)$, we can write the transport coefficients as

$$\eta = \frac{4T}{5\sigma_t}\left(1 + \frac{z^2}{20} + O\left(z^4\ln z\right)\right), \quad (4.20)$$

$$\zeta = \frac{mz^3}{108\sigma_t}\left(1 + O\left(z^5\ln z\right)\right), \quad (4.21)$$

where the transport cross section σ_t [46] is,

$$\sigma_t(\tilde{k}) = \int dt \frac{d\sigma_{el}}{dt}\frac{4t}{\tilde{k}}\left(1 - \frac{t}{\tilde{k}}\right). \quad (4.22)$$

The elastic gluon scattering matrix elements in deconfined systems are modeled by a Debye-screened form [47]

$$\frac{d\sigma_{el}}{dt} = \sigma_0(\tilde{k})\left(1 + \frac{\mu^2}{\tilde{k}}\right)\frac{\mu^2}{(t+\mu^2)^2}, \quad (4.23)$$

where,

$$\sigma_0(\tilde{k}) = \frac{9\pi\alpha_v 2(\tilde{k})}{2\mu^2}. \quad (4.24)$$

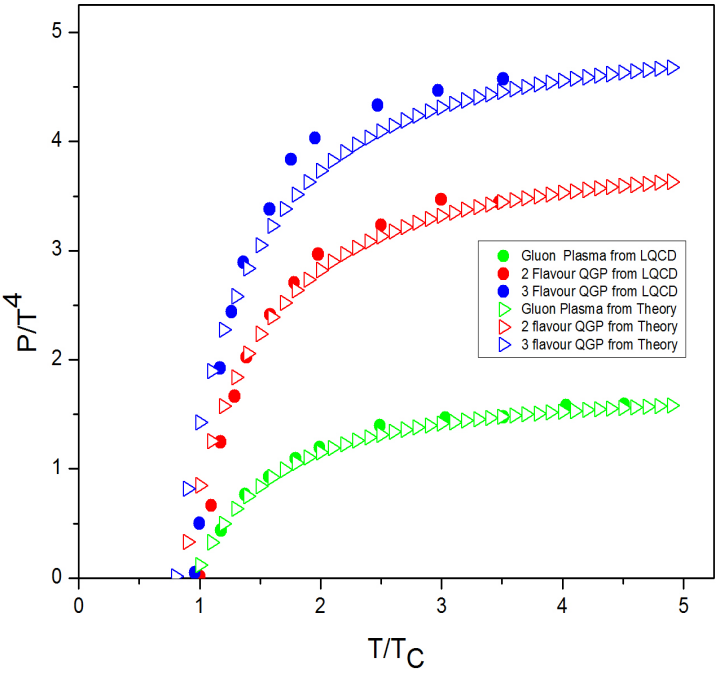

Figure 4.1: Pressure as a function of T/T_c, using Cluster expansion Theory (triangle) and lattice results (dots) for pure gauge (lower curve), two-flavor (middle curve), and three-flavor (upper curve) QGP.

it denotes the total cross section. Where $\alpha_v = \alpha_v(T)$ is the effective coupling constant and μ is the screening mass. Then the (4.22) becomes,

$$\sigma_t(\tilde{k}) = \sigma_0(\tilde{k}) 4\tilde{z}(1+\tilde{z})[(2\tilde{z}+1)\ln(1+\frac{1}{\tilde{z}}) - 2]. \tag{4.25}$$

We assume $\sigma_0(\tilde{k})$ to be energy independent and neglect its weak logarithmic dependence on $\tilde{k}$ in the energy range relevant at RHIC. We use the value of mean partonic Mandelstam variable $\tilde{k} \approx 17T^2$[48]. $\tilde{z} = \frac{\mu^2}{\tilde{k}}$, is a monotonic function of screening mass μ and has maximum value in the isotropic ($\mu \to \infty$) case. From perturbation theory one can obtain the dependence of coupling constant α_v and the screening mass μ, varies as $\mu^2 \approx 4\pi\alpha_v T^2$ for gluon system.

EoS of QGP and transport cross section should come within the same framework. The entropy density that we use was obtained by considering the modified Cornell potential as the interaction. The calculation of transport cross section can be made consistent with this by extracting the α_v in Eq.(4.24) from the same

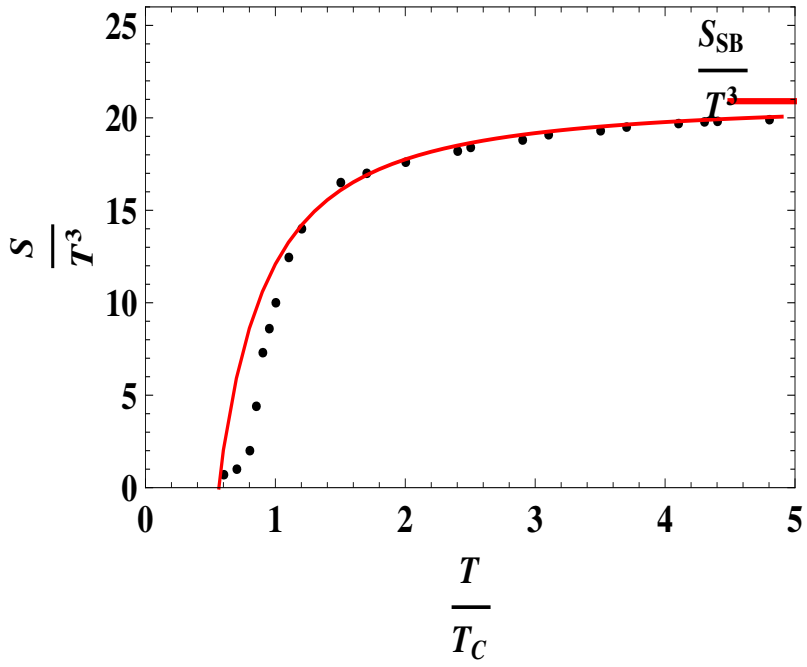

Figure 4.2: Entropy density as a function of temperature T, using Cluster expansion (CE) theory (solid red line), lattice results (black dots) [3] and SB limit(solid blue line)

interaction potential. The most convenient method of doing this is to find the QCD force,i.e. $\frac{dV(r)}{dr}$ [49] to obtain the running coupling α_{qq},

$$\alpha_{qq}(r,T) \equiv \frac{3}{4} r^2 \frac{dV(r)}{dr} \tag{4.26}$$

The running coupling $\alpha_{qq}(r,T)$ becomes maximum at a certain distance denoted by r_{max}. We fix the temperature dependent coupling constant, $\alpha_v(T) \equiv \alpha_{qq}(r_{max},T)$. For numerical estimates a specific form for $\alpha_v(T)$ has to be chosen. The choice of coupling constant in 2-flavor QCD and pure gauge theory are discussed [49, 50].

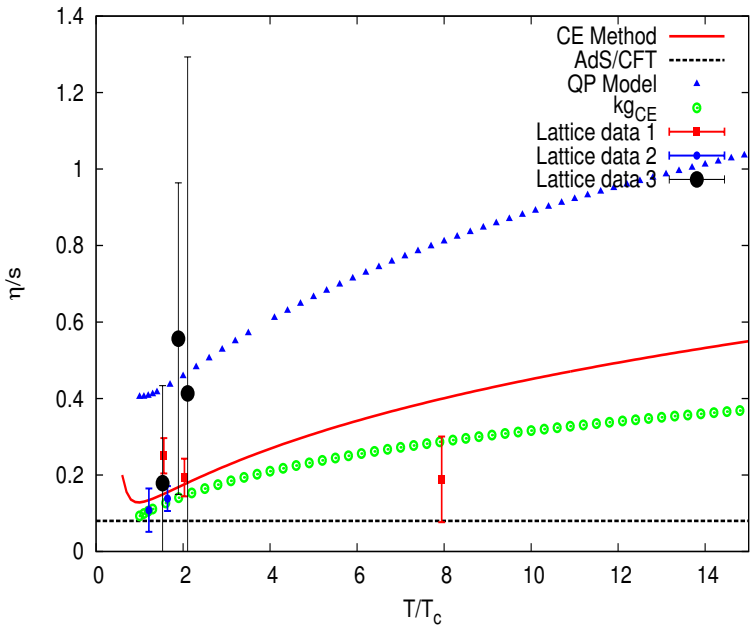

Figure 4.3: The ratio η/s in QGP for various temperature T. The red solid line represent the estimation of the η/s in QGP done in this paper, Green dotted line obtained rescaling g(T), Blue triangle line is QP model[4] and Black dotted line is AdS/CFT result from [9]. Symbols: full squares (Red) is lattice data 1[12], full circles (Black) is lattice data 2 [14] and full circles(Blue) is lattice data 3[11].

4.4 Results and Discussion

The ratio of the shear viscosity to the entropy density η/s and bulk viscosity to entropy density ζ/s has been calculated using Eqns. (4.11),(4.20),(4.21) and (4.25).

$$\frac{\eta}{s} = \frac{4T}{5\sigma_t s}, \tag{4.27}$$

and

$$\frac{\zeta}{s} = \frac{mz^3}{108\sigma_t s}. \tag{4.28}$$

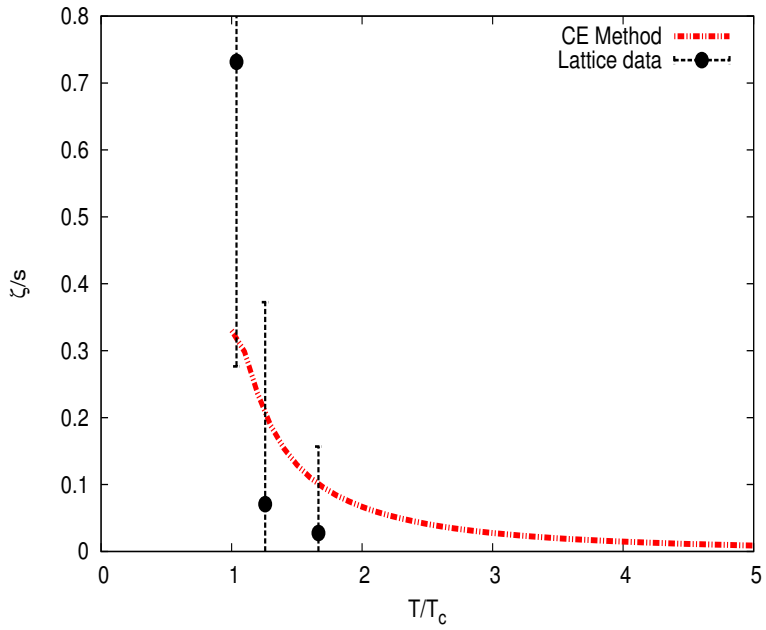

Figure 4.4: The ratio ζ/s as a function of temperature T, Red line represent the cluster expansion (CE) theory, full circles (Black) are lattice data[24].

We have plotted the pressure P (Fig.4.1) and entropy density s (Fig.4.2) using cluster expansion method and compared with LQCD results [3]. The shear viscosity to entropy density ratio η/s for the QGP at zero baryon chemical potential is presented in Fig. 4.3 (solid red line), blue triangle line is the result for the QP model [4], the symbols are different lattice QCD results [12, 14, 11] and the black dotted line indicates the Ads/CFT result [9]. The ratio η/s has a minimum value near the phase transition. This is expected because asymptotic freedom dictates that η/s increases with T in the deconfined phase since in this case the coupling between the quarks and the gluons (and the transport cross section) decreases logarithmically. The bulk viscosity to entropy density ratio ζ/s for QGP is plotted in Fig. 4.4, and it is compared with the lattice QCD results [24](Black full circle). It is the universal feature that the bulk viscosity coefficient has a prominent peak around the critical region.

We constrain the transport coefficients η/s and ζ/s by comparing theoretical predictions with the lattice data. In order to calculate the entropy density s, we have made an EoS, where the Mayer cluster expansion method was used with modified Cornell potential as the interaction among partons. Within QGP, this potential is color screened. We see that EoS gives a good fit with that of the lattice results. We try to clarify the detailed behaviour of the ratio η/s at the

transition (crossover) between hadron and quark-gluon phases. We find $\eta/s \approx 0.128$ at T_c which is very close to the theoretical lower bound. Furthermore, for temperatures $T \leq 1.8T_c$ the ratio η/s is in the range of the present experimental results at RHIC. The small η/s supports the success of the hydrodynamical description for QGP. When compared with η/s, the ζ/s decrease with increasing temperature for $T \geq T_c$. Together with experimental and phenomenological studies, the cluster expansion approach will enrich our understanding of the new state of matter.

Bibliography

[1] J. Adams et al. (STAR Collaboration), Nucl. Phys. A 757, 102 (2005).

[2] K. Aamodt et al. (ALICE), Phys. Rev. Lett. 105, 252302(2010).

[3] A. Bazavov et al. Phy. Rev. D 80, 014504 (2009).

[4] S. McDonald, C. Shen, F. Fillion-Gourdeau, S. Jeon, C. Gale, Phys. Rev. C 95, 064913 (2017)

[5] P. Romatschke, U. Romatschke, Phys. Rev. Lett. 99 (2007) 172301;

[6] M. Luzum, P. Romatschke, Phys. Rev. C 78 (2008) 034915.

[7] H. Song, U. Heinz, Phys. Lett. B 658 (2008) 279.

[8] G. Policastro, D. T. Son, and A. O, Starinets, Phys. Rev. Lett. 87, 081601 (2001).

[9] P. K. Kovtun, D.T. Son, A.O. Starinets, Phys. Rev. Lett. 94 (2005) 111601.

[10] R. A. Lacey et al., Phys. Rev. Lett. 98, 092301 (2007).

[11] L. P. Csernai, J I Kapusta, and L D McLerran, Phys. Rev. Lett. 97, 152303 (2006).

[12] H. B. Meyer, Phys. Rev. D 76, 101701 (2007).

[13] S. Sakai, A. Nakamura, PoS LAT 2007, 221 (2007).

[14] Astrakhantsev, N.Y., Braguta, V.V., Kotov, A.Y. J. High Energ. Phys. 101, (2017).

[15] A. Nakamura, S. Sakai, Phys. Rev. Lett. 94, 072305 (2005).

[16] D. Kharzeev and K. Tuchin, J. High Energy Phys. 0809, 093 (2008).

[17] F. Karsch, D. Kharzeev, and K. Tuchin, Phys. Lett. B663, 217 (2008).

[18] Akihiko Monnai, Tetsufumi Hirano, Nucl. Phys. A 830,471c (2009); Phys. Rev. C 80, 054906 (2009)

[19] Giorgio Torrieri, Boris Tomasik, Igor Mishustin Phys. Rev. C 77, 034903 (2008).

[20] Piotr Bozek, Phys. Rev. C 81, 034909 (2010).

[21] Arturo Avelino, Ulises Nucamendi, JCAP 1008, 006 (2010).

[22] Shou-wan Chen, Hui Dong, Qun Wang, J. Phys. G: Nucl. Part. Phys. 36, 064050 (2009).

[23] Massimo Mannarelli, Cristina Manuel, Phys. Rev. D 81, 043002 (2010); Xu-Guang Huang, Mei Huang, Dirk H. Rischke, Armen Sedrakian, Phys. Rev. D 81, 045015 (2010).

[24] Meyer H. B., Phys. Rev. Lett. 100, 162001 (2008).

[25] S. Mattiello and W. Cassing, Eur. Phys. J. C, 70: 243–249 (2010); S Mattiello, Physics of Atomic Nuclei, Vol. 75, No. 6, pp. 710–712 (2012).

[26] S. Mattiello and W. Cassing, J. Phys. G: Nucl. Part. Phys. 36 125003 (15pp) (2009).

[27] J. E. Mayer and M G Mayer, Statistical Mechanics (Wiley New York, 1977).

[28] R. K. Pathria, Pergamon International Library of Science, Engineering, Technology and Social studies, (1972).

[29] R. Balescu, Statistical mechanics of charged Particles (Inter science Publishers, Inc., New York, 1963).

[30] M. V. Ushcats, Phys. Rev. Lett. 109, 040601 (2012).

[31] M. V. Ushcats, J. Chem. Phys. 138, 094309 (2013).

[32] A. M. Syam Kumar, J P Prasanth, Vishnu M Bannur, Physica A 71-75, 432 (2015).

[33] V. M. Bannur, Physica A 419, 675–680 (2015).

[34] V. M. Bannur, Phys. Lett. B362, 7 (1995).

[35] K. M. Udayanandan, P Sethumadhavan, and V. M. Bannur, Phys. Rev. C 76, 044908 (2007).

[36] F. Karsch, M. T. Mehr, and H. Satz, Z. Phys. C 37, 617 (1988).

[37] B. Sheikholeslami-Sabzevari, Phys. Rev. C 65, 054904 (2002).

[38] Jiao-Kai Chen, Phys. Rev. D 86, 036013 (2012).

[39] G. S. Bali, Phys. Rev. D 62, 114503 (2000).

[40] F. Buisseret and C. Semay, V.mathieu, Eur. Phys. J. A 33, 87 (2007).

[41] A. Puglisi, S. Plumari, V. Greco, Physics Letters B 751, 326–330 (2015).

[42] V. M. Bannur, Eur. Phys. J. C50, 629–634 (2007).

[43] W. A. van Leeuwen, P. H. Polak, S. R. de Groot, Physics Letters A 37 (4), 323 – 324 (1971).

[44] W. A. Van Leeuwen, P. H. Polak, S. R. De Groot, Physica 63, 65–94 (1973).

[45] A. Wiranata, M. Prakash, Phys.Rev. C85, 054908 (2012).

[46] B. Zhang, M. Gyulassy and C. M. Ko, Phys. Lett. B455, 45 (1999).

[47] D. Molnar, M. Gyulassy, Nucl. Phys. A 697(2002) 495–520.

[48] A. Majumder, B. Muller, X.-N. Wang, Phys. Rev. Lett. 99, 192301 (2007).

[49] Olaf Kaczmarek, Felix Zantow, Phys. Rev. D 71, 114510 (2005).

[50] O. Kaczmarek, F. Karsch, F. Zantow et al., Phys. Rev. D 70, 074505 (2004).

Chapter 5

Semi-classical Equation of State of Quark-Gluon Plasma

5.1 Introduction

The experiments for creating the quark-gluon plasma (QGP) in Relativistic Heavy-Ion Collider (RHIC) at the BNL [1] and CERN Large Hadron Collider [2], conceived many properties of that state of matter. Many theoretical models have been formed to explore thermodynamics of QGP. In strongly interacting quark-gluon plasma model (sQGP) [3] the effects of the colored and colorless bound states hadron resonances are taken into account. In the quasi-particle QGP (qQGP) model [4, 5, 6], it is assumed that QGP is made up of quasi-particles with a temperature depended mass. The strongly coupled quark-gluon plasma model (SCQGP) [7, 8] considered that QGP is strongly coupled near the transition temperature T_c and used the equation of state (EoS) of strongly coupled quantum electrodynamic plasma (QED) with proper modifications for QCD.

The Cornell potential model for QGP based on Mayer's theory of plasma [9, 10] is also proposed in the same sense as in classical electrodynamical plasma. The CE method in plasma was taken into account and a detailed derivation of the equation of state and hence the transport coefficients of the QGP was calculated [23]. In this investigation, the Cornell potential between the partons in the

deconfined phase plays a crucial role to reproduce the EoS of the quark-gluon plasma. Mayer's cluster expansion method [18] is studied and the low-density limitation is considered in [29, 30] and finally an equation of state has been derived on the basis of the rigorous statistical approach in the high-density region for lattice gas in [31]. Quark-gluon plasma phase transition was studied using the cluster expansion method in [24], where a satisfactory result was obtained for the phase transition and region of condensation of QGP with the modified Cornell potential. In this paper we obtain the complete EoS for QGP using Cornell potential model and compare it with the lattice results [11],lattice6.

We formulate an equation of state of QGP using Mayer's CE method, in particular above the critical temperature T_c. Mayer's theory of plasma was described in [20], where one sums a certain set of infinite diagrams. A generalised equation of state of QGP was computed in [9, 10] using Mayer's theory of plasma. Their classical cluster expansion method is taken based on the assumption that for higher temperature, i.e, $T \geq 150MeV$ quantum effect can be neglected. Another argument for taking classical treatment is that at higher temperature the thermal wavelength is approximately in the range of nuclear forces. But the results deviate from lQCD results when T approaches T_c, where QGP is a strongly coupled system. We derive a semi-classical EoS including the quantum aspects in the low temperature region.

In [22] the authors try to develop a description of QGP by considering it as consisting of binary bound states, both hadronlike (colorless) and exotic (colored) bound pairs. Mayer's cluster expansion method has been employed in the quarkonia enhancement studies [25]. In this study, we have used the quantum cluster expansion to take into account the contribution of binary bound states in an effort to obtain a better fit with lattice data at temperatures near T_c.

5.2 Quantum EoS and Cluster Integral

The characteristic feature of quantum cluster expansion method [19] is to introduce cluster function $\hat{U}_l$. In the presence of interactions, we expect that the functions $\hat{U}_l$ would be quite appropriate for carrying out high temperature expansions. The partition function for the N particle system is,

$$Q_N(V,T) = \frac{1}{N!\lambda^{3N}} \int \grave{\sum_{\{m_l\}}} \left[\sum_p [U1...U2][U2...U2].. \right] d^{3N}r, \tag{5.1}$$

where the restricted summation goes over all the sets $\{m_l\}$ with the condition

$$\sum_{l=1}^{N} l m_l = N; \qquad m_l = 0, 1, 2... \tag{5.2}$$

The pressure and particle density of the non-ideal system in terms of the cluster integral b_l in the limit $V \to \infty$ is,

$$\frac{P}{T} = \frac{1}{\lambda^3} \sum_{l=1}^{\infty} b_l(T) z^l \tag{5.3}$$

$$n = \frac{1}{\lambda^3} \sum_{l=1}^{\infty} l b_l(T) z^l \tag{5.4}$$

where $b_l(T) \equiv \lim_{V\to\infty} b_l(V,T)$, z is the fugacity and $\lambda = \sqrt{\frac{2\pi}{mT}}$ is the thermal wave length.

The partons only form cluster and there is no change in the particle number of the system, hence the chemical potential of the system is taken to be zero. Consider up to second term in the Eq.(5.3), Eq.(5.4) and combine the equations, we get,

$$\frac{P}{T} = n_1 + \frac{n_{B2}}{2}, \tag{5.5}$$

where $n_1 = \frac{b_1}{\lambda^3}$ and $n_{B2} = \frac{2b_2}{\lambda^3}$.

The cluster integral b_l in the cluster expansion method includes the interac-

tion potential between the partons, the Cornell potential. The cluster integrals are defined in terms of the trace of the l-body cluster operator U_l,

$$b_l(V,T) = \frac{1}{l!\lambda^{3(l-1)}V}\int U_l(r_1, r_2, r_3, ..., r_l)d^{3l}r \tag{5.6}$$

Let us represent cluster integral as the sum of two terms,

$$b_l = b_l^{(0)} + b_l^{(i)}, l > 1. \tag{5.7}$$

Where $b_l^{(0)}$ are the cluster integral for the ideal system and $b_l^{(i)}$ appear due to the particle interaction

$$b_1 = 1, \tag{5.8}$$

$$b_2 = \frac{1}{2\lambda^3 V}\left(\sum_i e^{(-\beta E_i^{(2)})} - \sum_i e^{(-\beta E_i^{(0)})}\right), \tag{5.9}$$

where $E_i^{(2)}$, $E_i^{(0)}$ are the energy states of the two particle system, with and without interaction, respectively.

By separating the different angular momenta and the possible discrete states from the continuum states, Eq.(5.6) can be transformed into

$$\begin{aligned} b_2 - b_2^{(0)} = \; & 8^{(1/2)}\sum_B e^{-\beta E_B} + \frac{8^{(1/2)}}{\pi}\sum_l{}'(2l+1) \\ & \int_0^\infty e^{-\beta\hbar^2k^2/m}\frac{\partial\eta_l(k)}{\partial k}dk \end{aligned} \tag{5.10}$$

for bound states

$$b_2 - b_2^{(0)} = 8^{(1/2)}\sum_B e^{-\beta E_B} \tag{5.11}$$

The value of $b_2^{(0)}$ is $-\frac{1}{2}^{(5/2)}$ for Fermions and $+\frac{1}{2}^{(5/2)}$ for Bosons.

The cluster integral b_l may be related to irreducible cluster integral β_l using

Lagrange's theorem [19] via,

$$\beta_{l-1} = \sum_{\{m_k\}}{}' (-1)^{\sum_k (m_k-1)} \frac{(l-2+\sum_k m_k)!}{(l-1)!} \prod_k \frac{(kb_k)^{m_k}}{m_k!} \tag{5.12}$$

where the restricted summation is with the condition,

$$\sum_{k=2}^{l} (k-1)m_k = l-1; \qquad m_k = 0, 1, 2... \tag{5.13}$$

5.3 EoS of QGP using Mayer's Theory of CE

According to Mayer's theory of classical plasma [20], the equation of state for any plasma is given by

$$\frac{P}{T} = \sum_i n_i + D - \sum_i n_i \frac{\partial D}{\partial n_i}, \tag{5.14}$$

in natural units. For gluons plasma let the number density n_i be represented by n_g and for quarks-antiquarks plasma n_q, $n_{\bar{q}}$ respectively. D is the sum over all irreducible cluster integrals $\beta_{(N_i N_j)}$ and is defined as

$$D = \sum_{N \geq 2} \sum_{N_i} \sum_{N_j} \beta_{(N_i N_j)} n_i^{N_i} n_j^{N_j} \tag{5.15}$$

where $N = N_i + N_j$. D can be simplified as follows after using Newton's binomial formula,

$$D = \frac{1}{4\pi^2} \int_0^\infty l^2 dl \left[\frac{(-\kappa^2 V_l)^2}{2} + \frac{(-\kappa^2 V_l)^3}{3} + ... \right] \tag{5.16}$$

The Inverse Debye length squared varies as $\kappa^2 = \frac{n_g}{T}$ and $\kappa^2 = \frac{n_q + n_{\bar{q}}}{T}$ for gluon plasma and quark-antiquark plasma respectively. Then Eq.(5.14) becomes,

$$\frac{P}{T} = \kappa^2 T + D - \kappa^2 \frac{\partial D}{\partial \kappa^2} \tag{5.17}$$

Thus the EoS for both plasma has the same appearance with different values for κ^2.

Here the summation goes over any two vertices and is connected by at least two distinct path which followed the lines in the diagrammatic approach. But the simply connected two vertex diagrams such as β_{11},β_{20} and β_{02} are excluded from the summation [20].

We want to include the quark and gluon bound states that exist in the strongly coupled region of the QGP [22]. Hence we formulated a modified CE (mCE) theory in plasma by combining Eq.(5.14) and second term in Eq.(5.5). Thus we obtained a semi-classical EoS of QGP as given below,

$$\frac{P}{T} = \sum_i n_i + \frac{1}{2}\sum_i n_{B_{2i}} + D - \sum_i n_i \frac{\partial D}{\partial n_i} \tag{5.18}$$

where the number density of bound state quarks and gluons is represented by $n_{B_{2q}}$ and $n_{B_{2g}}$ respectively. To get a simplified EoS, we introduced a new parameter $\eta^2 = \frac{\beta_{11}}{2} T_c^{1/2} \left(\frac{m}{2\pi}\right)^{3/2}$ by considering (5.5) and (5.12). The bound state contribution become less at high temperature regime, it is also considered in the term η^2. Then the (5.18) becomes,

$$\frac{P}{T} = \kappa^2 T + \eta^2 T + D - \kappa^2 \frac{\partial D}{\partial \kappa^2} \tag{5.19}$$

Here we made a quantum correction in the EoS of QGP by including bound states of quarks and gluons. To evaluate the sum, we first differentiated D with respect to κ^2, we then found a geometric progression

$$\frac{\partial D}{\partial \kappa^2} = \frac{\kappa^2}{4\pi^2} \int_0^\infty l^2 dl \frac{\kappa^2 V_l}{1 + \kappa^2 V_l} \tag{5.20}$$

where V_l is the interaction potential in momentum space. Here the interaction potential between the constituents described by Cornell potential [10, 26, 27],

$$\grave{V}(r_{ij}) = \left(\frac{\alpha}{r_{ij}} - \sigma r_{ij}\right) \tag{5.21}$$

contains the coulomb plus an additional linear term. $\alpha = \frac{4\alpha_s}{3}$ for quark-antiquark plasma and $\alpha = 3\alpha_s$ for gluon plasma, where α_s is the strong coupling constant of the color Coulomb potential and σ is the string tension. The Casimir scaling ($C = 9/4$) has been included in the potential of gluon plasma for obtaining an exact EoS of QGP [32, 33].

The interaction potential in plasma is generally defined as, $V(r,T) = z_i z_j \acute{V}(r_{ij})$, where $z_i = 1$ or $z_i = -1$ if the particle is quark or antiquark respectively.

Take the Fourier transform of Eq.(5.21) for quark anti-quark plasma and gluon plasma separately is given by,

$$V_{lq\bar{q}} = \frac{16\pi\alpha_s}{3(l^2+k^2)} + \frac{8\pi\sigma}{(l^2+k^2)^2} \tag{5.22}$$

$$V_{lg} = \frac{12\pi\alpha_s}{(l^2+k^2)} + \frac{18\pi C\sigma}{(l^2+k^2)^2} \tag{5.23}$$

The constant k is the convergence parameter which will take the value zero at the end of the calculation. Substitute Eq.(5.22) and Eq.(5.23) in Eq.(5.20) and integrating over l gives $\frac{\partial D}{\partial \kappa^2}$ and integrating $\frac{\partial D}{\partial \kappa^2}$ over κ^2, we get D.

Adding number density contributions of quarks and gluon gives the equation of state of state. For quark-antiquark plasma,

$$n_q + n_{\bar{q}} \approx \frac{12n_f}{\pi^2}T^3 \sum_{l=1}^{\infty} \frac{(-1)^{l-1}}{l^3} = \frac{12n_f}{\pi^2}T^3 \frac{3}{4}\zeta(3) \tag{5.24}$$

Where n_f is the number of flavours of the quark anti-quark plasma.

For gluon plasma,

$$n_g \approx \frac{g_I}{\pi^2} T^3 \sum_{l=1}^{\infty} \frac{1}{l^3} = g_I T^3 \frac{\zeta(3)}{\pi^2} \tag{5.25}$$

Where g_I=16 is the internal degrees of freedom for gluons and $\zeta(3)$=1.202 is the Riemann-zeta function.

Solution of the Cornell Potential

To evaluate the n_B in Eq.(5.18), we want to find the a solution of Schrodinger equation with Cornell potential. The Cornell Potential does not admit exact solutions to the Schrodinger equation. So we use the Nikiforov–Uvarov Method to find an approximate solution [21, 34].

The non-relativistic radial Schrodinger equation for the quark and antiquark system is given by,

$$\frac{1}{r^2}\frac{d}{dr}\left[r^2 \frac{dR_{nl}(r)}{dr}\right] + \left(2\mu\left[E - V(r)\right] - \frac{l(l+1)}{r^2}\right) R_{nl}(r) = 0. \tag{5.26}$$

Where the $V(r)$ is the Cornell potential between the partons and μ is the reduced mass and r is the relative coordinate. Introduced the reduced radial wave function $\phi_{nl}(r) = rR_{nl}(r)$ and is normalized by the condition $\int_0^\infty |\phi_{nl}(r)|^2 dr = 1$. Apply Eq.(5.21) in Eq.(5.26) and making the change of variable $x = 1/r$, equation becomes,

$$\frac{d^2(\phi_{nl}(r))}{dx^2} + \frac{2x}{x^2}\frac{d(\phi_{nl}(x))}{dx} + \frac{2\mu}{x^4}\left[E - \frac{\sigma}{x} + \alpha x - \frac{l(l+1)x^2}{2\mu}\right]\phi_{nl}(x) = 0 \tag{5.27}$$

Let us assume that there is a characteristic radius r_0 of the quark anti-quark system. An approximation scheme on $\frac{\sigma}{x}$ is based on the power series expansion around r_0, i.e. around $\delta \equiv \frac{1}{r_0}$.

$$\frac{\sigma}{x} = \frac{\sigma}{\delta^3}\left[3\delta^2 - 3\delta x + x^2\right] \tag{5.28}$$

$$\frac{d^2(\phi_{nl}(r))}{dx^2} + \frac{2x}{x^2}\frac{d(\phi_{nl}(x))}{dx} + \frac{2}{x^4}\left[-a + bx - cx^2\right]\phi_{nl}(x) = 0 \tag{5.29}$$

where $a = -\mu\left[E - \frac{3\sigma}{\delta}\right]$, $b = \mu\left[\alpha + \frac{3\sigma}{\delta^2}\right]$ and $c = \mu\left[\frac{l(l+1)}{2\mu} + \frac{\sigma}{\delta^3}\right]$.

Consider the differential equation [21],

$$u'' + \frac{\bar{\tau}(r)}{\gamma(r)}u' + \frac{\bar{\gamma}(r)}{\gamma^2(r)}u = 0 \tag{5.30}$$

where $\bar{\tau}$ is the polynomial of first degree, γ and $\bar{\gamma}$ are the polynomial, at most second degree. Comparing Eq.(5.30) with Eq.(5.29), we get $\bar{\tau} = 2x$, $\gamma = x^2$ and $\bar{\gamma} = 2(-a + bx - c^2)$

Apply Nikiforov–Uvarov method, by solving Eq.(5.29) we obtain an approximate solution,

$$E_{nl} = \frac{3\sigma}{\delta} - \frac{2\mu(\alpha + \frac{3\sigma}{\delta^2})^2}{\left[(2n+1) \pm \sqrt{1 + 4l(l+1) + \frac{8\mu\sigma}{\delta^3}}\right]^2} \tag{5.31}$$

The corresponding wave function $R_{nl}(r)$,

$$R_{nl}(r) = N_{nl} r^{\frac{-b}{\sqrt{2a}}-1} e^{\sqrt{2a}r}\left(-r^2\frac{d}{dr}\right)^n r^{-2n+\frac{2b}{\sqrt{2a}}} e^{-2\sqrt{2a}r} \tag{5.32}$$

where N_{nl} is the normalization constant.

Apply Eq.(5.31) in to the Eq.(5.11) and we get η^2. The other thermodynamic quantities can be calculated from Eq.(5.19) using thermodynamic relations.

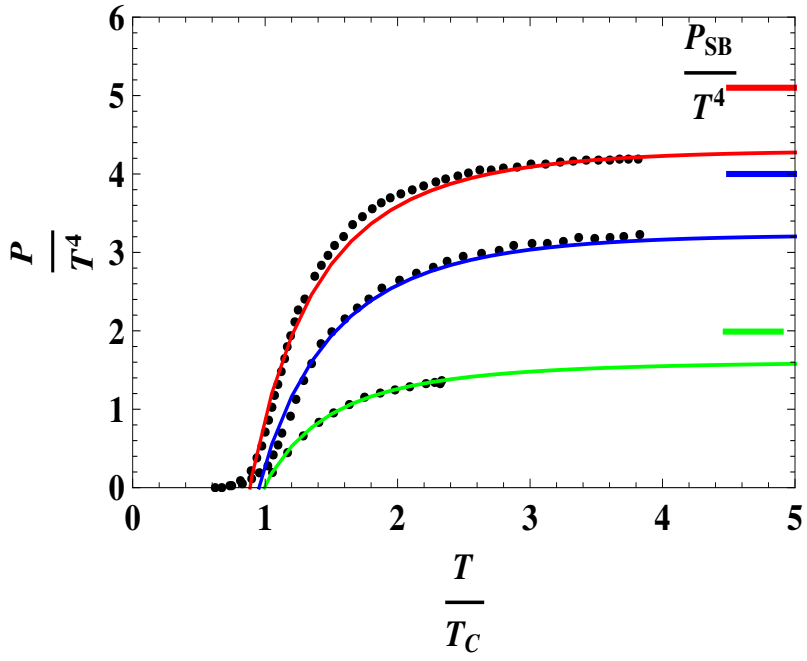

Figure 5.1: The ratio P/T^4 for various temperature T is plotted. The solid lines represent the estimation of the P/T^4 in QGP using CE method (Red line $\rightarrow$ three flavor QGP, Blue line $\rightarrow$ two flavor QGP and Green line $\rightarrow$ pure gauge). The black full circles is the lQCD results [12].

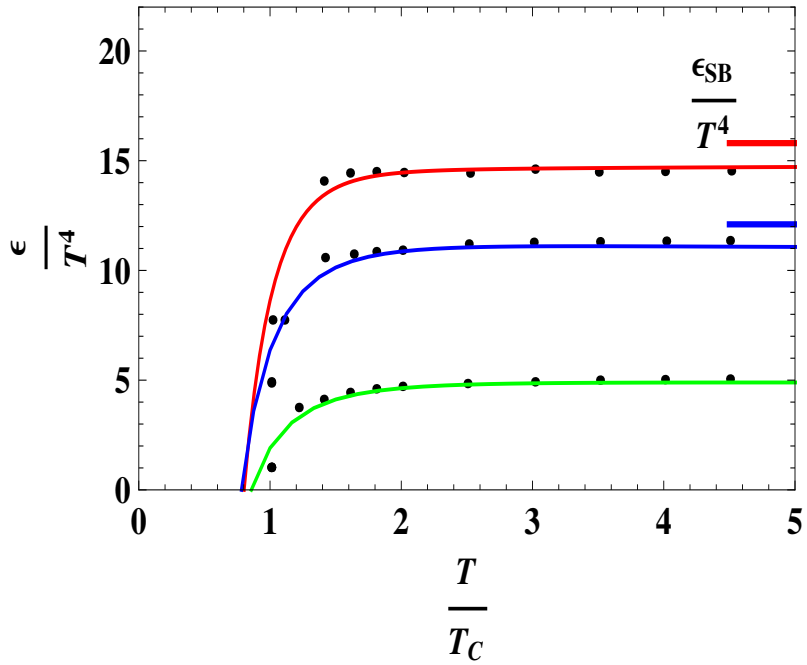

Figure 5.2: The ratio ϵ/T^4 for various temperature T is plotted. The solid lines represent the estimation of the ϵ/T^4 in QGP using CE method. Red, Blue and Green lines represent the three flavor QGP, two flavor QGP and pure gauge respectively. The black full circles is the corresponding lattice data [12].

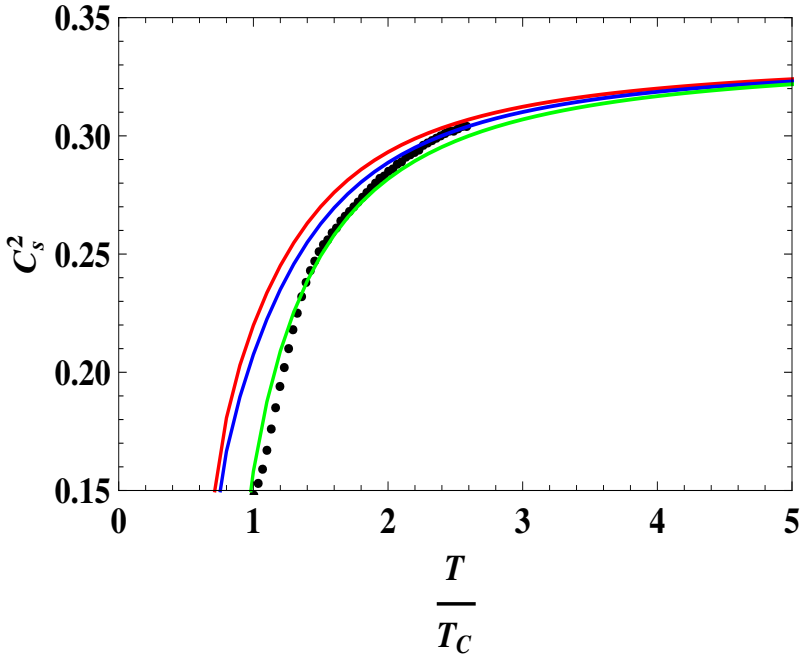

Figure 5.3: The C_s^2 verses T/T_c is plotted. The solid lines represent the square of the velocity of sound using CE method, Red, Blue and Green lines are for three flavor, two flavor and pure gauge respectively. The Black full circles is the lQCD results for pure gauge [16].

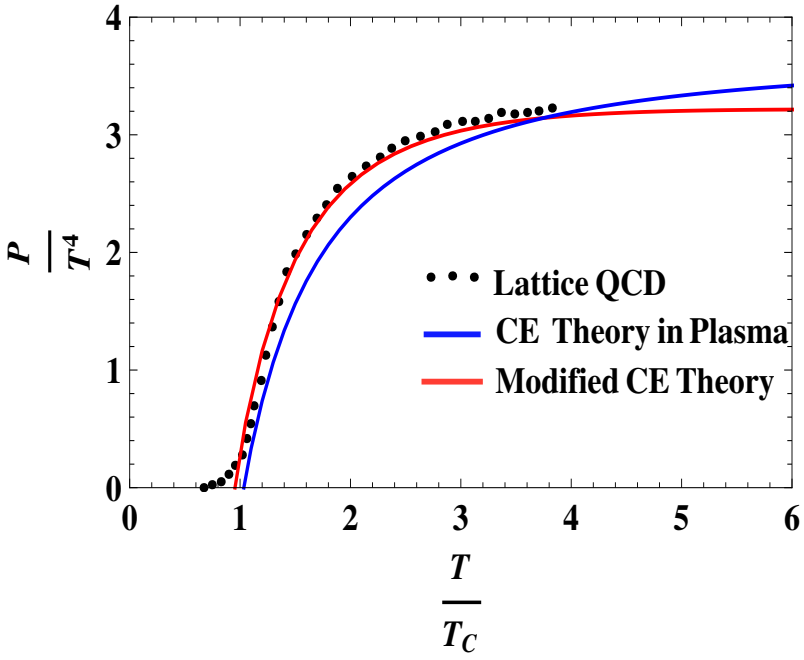

Figure 5.4: The comparison of our modified CE theory with CE theory of plasma [10]. The black full circles is the corresponding lattice data [12].

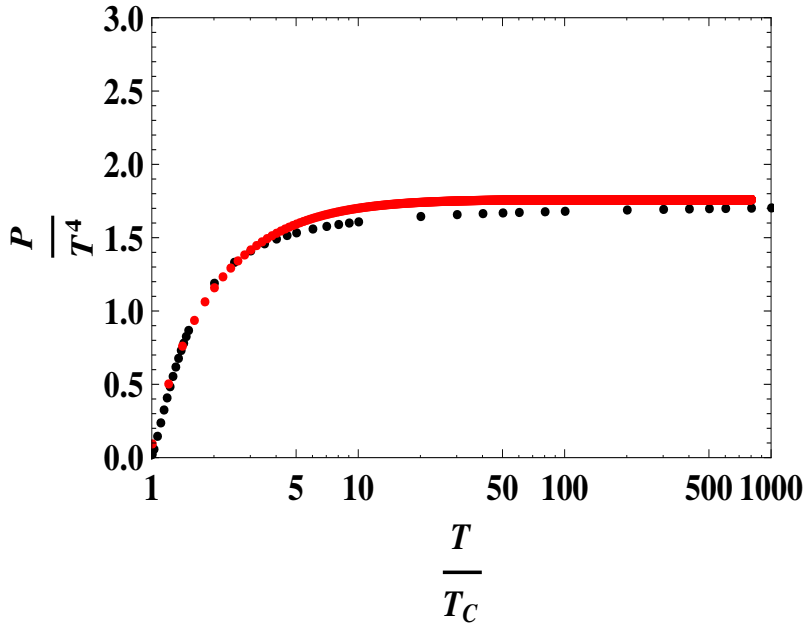

Figure 5.5: P/T^4 upto $1000T_c$ is plotted (T/T_c is in 'Mathematica' logarithmic scale). The black full circles is the corresponding lattice data. [17].

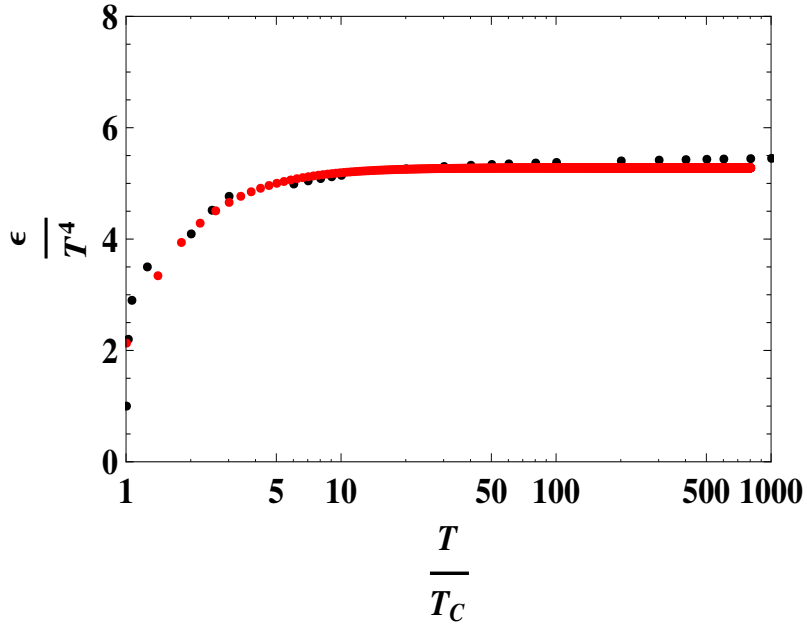

Figure 5.6: ϵ/T^4 upto $1000T_c$ is plotted. The black full circles is the corresponding lattice data [17].

5.4 Results and Discussion

The modified EoS fits the lattice data [11]-[16] on the gluon plasma, and 2-flavor, 3-flavor QGP. In Fig.5.1 we have plotted the P/T^4 versus T/T_c for three flavor, two-flavor, and pure gauge QGP along with lattice results. For each system, the σ, α_s and δ are adjusted, so that we get a good fit with the lattice results. Our EoS fit with the lattice QCD results for $\alpha = 0.12$, 0.1 and 0.09 and $\sigma = 0.34$ GeV^2, 0.75 GeV^2 and 0.8 GeV^2 for gluon plasma, two flavor, three flavor QGP respectively. The parameter $\delta = 0.6$, 0.69 and 0.84 for gluon, two and three flavor system and the number n takes values 0,1,2, etc and is related to the principal quantum number $\hat{n}$ via $\hat{n} = n + l + 1$ [34]. We take critical temperature $T_c = 275$ MeV, 175 MeV and 155 MeV respectively for the gluon plasma, and 2-flavor, 3-flavor QGP.

In Fig.5.2 we plot ϵ/T^4 versus T/T_c for all three systems along with the lattice results. Our new EoS matches with the lattice EoS at all temperature region. This is because we have included bound states of quark and gluons, which exist very close to T_c. We found that the fitting is not good near $T = T_c$ in the previous paper [9, 10], where the QGP may be a strongly interacting plasma. The quantum nature is needed to express the behaviour of QGP in the strongly coupled region. Here we address the problem by deriving a semi-classical EoS for the system and get a considerably good fit with lqcd results.

The velocity of sound plays an important role in the hydrodynamical evolution of the matter created in the heavy-ion collision, especially in the freeze-out stage. The functional relation between pressure P and the energy density ϵ with the square of the velocity of sound via $C_s^2 = \frac{\partial P}{\partial \epsilon}$. The $C_s^2 = 1/3$ for an ideal gas. In Fig.5.3 we plotted the square of the velocity of sound with T/T_c and compared with lattice QCD results.

The energy density and pressure of gluon plasma upto $1000T_c$ are plotted in Fig.5.5, Fig.5.6, using our modified version of Mayer's theory of plasma. The thermodynamic parameters will reach the Stefan-Boltzmann limit at high temperature scale and we get good fit with lattice QCD results at all temperature

range [17].

The comparison of our modified version of cluster expansion theory with cluster expansion theory of K.M. Udayanandan et al.,[10] is plotted in Fig.5.4. We observe the semi-classical description of EoS well fit with the lattice QCD results [12], because here we taking the light quark quantum effects in the strongly interacting QGP.

We revisited the equation of state of QGP using Cornell potential and compared theoretical results with the lattice data. In order to calculate the pressure P and energy density ϵ we have made an equation of state in a semi-classical way using Mayer's theory of plasma. We include the behaviour of bound states of quarks and gluon by deriving a complete equation for quark-gluon phases. We found that the bound state of partons, i.e, qq and gg occurs in the temperatures of the order of a few times the critical temperature $T = 1$–$3T_c$ and it is evident in the present experimental results at RHIC. We plotted P/T^4, ϵ/T^4 and C_s^2 for varies temperature range. The fit of the EoS with lattice QCD results in all temperature region is the success of our semi-classical description for quark-gluon plasma EoS. Together with experimental and phenomenological studies, the Cornell potential approach will enrich our understanding of the new state of matter.

Bibliography

[1] J. Adams et al. (STAR Collaboration), Nucl. Phys. A 757, 102 (2005).

[2] K. Aamodt et al. (ALICE), Phys. Rev. Lett. 105, 252302 (2010).

[3] E. Shuryak, Nucl. Phys. A750, 64 (2005).

[4] V. M. Bannur, Phys. Lett. B 647, 271 (2007).

[5] V. M. Bannur, Eur. Phys. J. C 50, 629 (2007).

[6] P. Simji and V. M. Bannur, International Journal of Modern Physics A 28, 1350121 (2013).

[7] V. M. Bannur, J. Phys. G: Nucl. Part. Phys. 32, 993 (2006).

[8] Boris A. Gelman, Edward V. Shuryak and Ismail Zahed, Phys. Rev. C 74, 044908 (2006).

[9] V. M. Bannur, Phys. Lett. B 362, 7 (1995).

[10] K. M. Udayanandan, P. Sethumadhavan, and V. M. Bannur, Phys. Rev. C 76, 044908 (2007).

[11] F. Karsch, E. Laermann, A. Peikert, Physics Letters B 478, 447–455 (2000).

[12] F. Karsh, Nucl. Phys. A, 698, 199 (2002).

[13] E. Laermann.,O. Philipsen, Ann. Rev. Nucl. Part. Sci., 53, 163 (2003).

[14] Y. Aoki, Z. Fodor, S. D. Katz, and K. K. Szabo, J. High Eenrgy Phys. 01, 089 (2006).

[15] C. Bernard et al. Phys. Rev. D 75, 094505 (2007).

[16] A. Bazavov et al.Phys. Rev D 90, 094503 (2014).

[17] Sz. Borsanyi et al., arXive:1204.6184[hep-lat].

[18] J. E. Mayer and M. G. Mayer, Statistical Mechanics (Wiley New York, 1977).

[19] R. K. Pathria, Statistical Mechanics, Butterworth-Heinemann, Oxford, 1997

[20] R. Balescu, Statistical mechanics of charged Particles (Inter science Publishers, Inc., New York, 1963).

[21] Nikiforov, A. F and Uvarov, V. B, Special Functions of Mathematical Physics (Birkhauser, Basel)(1988).

[22] E. V. Shuryak and Ismail Zahed, Phys. Rev. D 70, 054507 (2004).

[23] Prasanth. J. P, V. M. Bannur, Physica A 498, 10–16 (2018).

[24] A. M. Syam Kumar, J. P. Prasanth, Vishnu M Bannur, Physica A 71-75, 432 (2015).

[25] B. Sheikholeslami-Sabzevari, Phys. Rev. C 65, 054904 (2002).

[26] F. Karsch, M. T. Mehr, and H. Satz, Z. Phys. C 37, 617 (1988).

[27] Matthias Doring, Kay Hubner, Olaf Kaczmarek, and Frithjof Karsch, Phys. Rev. D 75, 054504 (2007).

[28] Jiao-Kai Chen, Phys. Rev. D 86, 036013 (2012).

[29] M.V.Ushcats, Phys. Rev. Lett 109, 04060190(2012).

[30] M.V.Ushcats, Phy. Rev. E 87,042111 (2013).

[31] M.V.Ushacats, Phys. Rev. E 91, 052144 (2015).

[32] G. S. Bali, Phys. Rev. D 62, 114503 (2000).

[33] F. Buisseret and C. Semay, V.mathieu, Eur. Phys. J. A 33, 87 (2007).

[34] Y. Cançelik and B. Gönül, Modern Physics Letters A 29, 32 (2014).

Chapter 6

Conclusions and Future Plan

In this work, we have conducted a study to develop the statistical mechanics and thermodynamics of QGP based on cluster expansion method. Particle collisions in laboratories recreating the QGP reveal that, the early universe was filled with droplets of this primordial soup. The data coming from the different laboratories are the ballpark of what different theories predicted for QGP existence. The prediction of different theories depends on what method they include. Our cluster expansion method will help us to study the signature of QGP, equation of state and the transport coefficients of QGP.

The Mayer's method of cluster expansion helps us to develop an EoS for non-ideal quark-antiquark plasma under non-relativistic approximation. This approach allows us to take into account the fundamental interactions among the quarks via Cornell potential. Study of quarkonium dissociation and strangeness enhancement will enrich our understanding about the signature of QGP in relativistic heavy ions collisions. On the footing of the Mayer's cluster expansion method, a study has been performed and the criterion obtained for the temperature, where heavy quarkonium like charmonium ($J/\psi(c,\bar{c})$) and bottomonium ($\Upsilon(b,\bar{b})$) suppression occurs. The earlier finding was based on grand canonical partition function of the system, which ignored the limitations of the restrictive summation $\sum_{l=1}^{N} lm_l = N$. Our present study is based on canonical partition function of the system and helps to eliminate such deficiencies. The EoS using screened Cornell potential shows the dissociation of heavy quarkonium J/Ψ and

Υ at the temperature range $T = 0.15 - 0.3GeV$. Our EoS is applicable to different species of quark system. The clustering of strange quarks in the phase transition region is considered and the multi-strange hadronisation has been investigated. We have obtained the EoS for $\Phi(s\bar{s})$ and $\Omega^{-}(sss)$ etc., and studied muti-strange hadronisation process. From the graph of different species of quark system, it is evident that a pronounced maximum number density occurs near the critical temperature T_c. The number density of different strange droplets are tabulated in Chapter 2. The main advantage of the cluster expansion method is that, we can apply the classical particle picture to the quarks.

This approach leads to exact results, when we apply it to the low density region. If we attempt to include condensation at high density region into our study, we encounter serious difficulties relating to the convergence of the summation over l and volume dependence of cluster integral b_l. The limitations of Mayer's EoS at condensation point in the high density regime is addressed by Ushcats. He has succeeded in deriving an EoS which is applicable for all density regions.

The study of hadron to QGP phase transition using modified Cornell potential is presented in Chapter 3. The earlier study of QGP and phase transition using cluster expansion method mainly focused on the high temperature and zero chemical potential. The new approach will enrich our understanding of deconfinement under high baryon density. We have taken into account the cluster expansion EoS for finite size system (fEoS) and EoS in the thermodynamic limit (CEEoS), which is extended into the high density region. The interaction models like Cornell potential model, including both attraction and repulsion, have indicated the adequacy of virial EoS in all density regions. The critical point where the system converges has been calculated for different temperatures. The region of convergence has been plotted for different number of particles, which shows that as the number of particle N increases, the high density interval of isotherms becomes more flat. A comparative study between Mayer's EoS and Ushcats EoS has been done for modified Cornell potential.

The perfect fluidity of the strongly-coupled QGP has been reported at RHIC. In these experiments we see a pronounced minimum in the value of shear viscosity near the critical temperature T_c. In relation to this, the novel notion of strong QGP has been put forward, and strong coupling properties of the QGP near the transition temperature T_c have been studied. Therefore, the inclusion of interactions between partons is mandatory to consistently describe the QGP in the region close to T_c. The lattice QCD results of the anisotropic flow of QGP is successfully explained QGP as a viscous fluid with $\eta/s \approx 0.1$. Some theorists are working to develop the theory of transport coefficient of QGP via computational techniques using QCD to perform reliable simulations. Mattiello et al., tried to develop the QCD EoS and hence the viscosity under the mathematical treatment of virial expansion. We estimate the transport coefficient of QGP more realistically based on cluster expansion theory of plasma.

We derived the EoS using modified Cornell potential based on Mayer theory of plasma. To calculate the transport coefficients, we used the Chapman-Enskog method. It provide a strong relationship between transport cross section and the interaction potential between the partons near T_c. In Chapter 4, the ratio of shear viscosity to entropy density (η/s) and ratio of bulk viscosity to entropy density (ζ/s) are derived and compared with the lattice QCD results. To derive a consistent relation, the coupling constant α_s is extracted from screened Cornell potential. We found that $\eta/s \approx 0.128$ at T_c, which is very close to the theoretical lower bound value of the AdS/CFT. Furthermore, for temperatures $T \leq 1.8T_c$ the ratio η/s is in the range of the present experimental results at RHIC. It confirms that QGP is a strongly coupled system near the critical temperature. When compared with our results, lattice QCD simulations also suggest that ζ/s is strongly enhanced near T_c, although the shear viscosity coefficient is suppressed. Considering the fact that the fluid dynamics slows down near T_c due to the small sound velocity C_s, the critical behaviour of η/s may play a crucial role on QGP dynamics.

The Mayer's theory of ionic plasma is briefly sketched in our work.

The outline is based on the derivation of equilibrium theory of imperfect gases. In the fifth chapter we extended this theory into QGP with proper modifications. Based on this theory V.M.Bannnur and K.M. Udayanandan have already derived a classical EoS for QGP. They ignored the contribution of bound states of quarks and gluons near the phase transition region as suggested by E.V.Shuryak et al. Moreover, the lowest order irreducible cluster integral β_{11} is not included in the EoS. We want to overcome mathematical limitations of this EoS to include the two particle bound states. We derived semi-classical EoS based on Mayer theory of plasma and included the quantum effects of liqht quark bound states near the transition region.

The bound state of partons occurs in the temperatures range $T = 1 - 3T_c$ and it is evident in the present theoretical calculations. We plotted different thermodynamic parameters such as, P/T^4, ϵ/T^4 and C_s^2 for various temperature range using our modified EoS. The fit of the EoS with lattice QCD results in all temperature region is the success of our semi-classical description of EoS. The energy density and pressure of gluon plasma upto $1000T_c$ are plotted using our modified version of Mayer's theory of plasma. Here the thermodynamic parameters reach Stefan-Boltzmann limit at high temperature scale and we get good fit with lattice QCD results at all temperature range. The comparison of our modified version of cluster expansion theory of QGP with cluster expansion theory of K.M. Udayanandan et al., is plotted. We observed the semi-classical description of EoS fits well with the lattice QCD results.

Future Work

Cluster expansion method will open the doors to study the quarkonium suppression using quantum cluster expansion. To calculate QGP equation of state and to incorporate lighter quarks, we should extend our work into relativistic and quantum regime. The advanced mathematical method of Lee and Yang will enrich the conceptual background of thermodynamics of QGP. Cluster expansion method in conjunction with medium modified potential will enable to arrive at the medium properties of QGP. Modification of our first work, provides the possibility to incorporate fourth cluster integral in cluster of four particle droplet (four-quark matter), which may provide evidence for a strange particle, called $Z_c(3900)$ [1, 2].

The incorporation of cluster expansion method and Yukawa potential, will lead to the mathematics of Clustering of Nuclei. Equation of state for QGP using cluster expansion method under finite chemical potential may leads to a complete understanding of the phase diagram. To invigorate the study of transport coefficients of quark-gluon plasma, we can derive EoS using the quantum cluster expansion method under finite chemical potential.

Bibliography

[1] M Ablikim et al.(BESIII Collaboration), Phys.Rev.Lett.**110** (2013) 252001.

[2] Z Q Liu et al.(Belle Collaboration), Phys.Rev.Lett.**110** (2013) 252002.

Appendix A

Bipolar Coordinates

Evaluate C_3 based on bipolar coordinate integration, by fixing the positions of the particle 1 and 2 and particle 3 takes all possible position. Rotation of the element of area $dxdy$ about the x axis sweeps out d^3r_{13} (see Fig.A.1), so that

$$d^3r_{13} = 2\pi y dx dy \tag{A.1}$$

The coordinates x and y can be transformed in terms of r_{13} and r_{23} using the Jacobian transformation, we get

$$dxdy = \frac{r_{13}r_{23}}{yr_{12}} dr_{13}dr_{23} \tag{A.2}$$

$$d^3r_{13} = \frac{2\pi r_{13}r_{23}}{r_{12}} dr_{13}dr_{23} \tag{A.3}$$

where $r_{13}^2 = x^2 + y^2$ and $r_{23}^2 = y^2 + (r_{12} - x)^2$

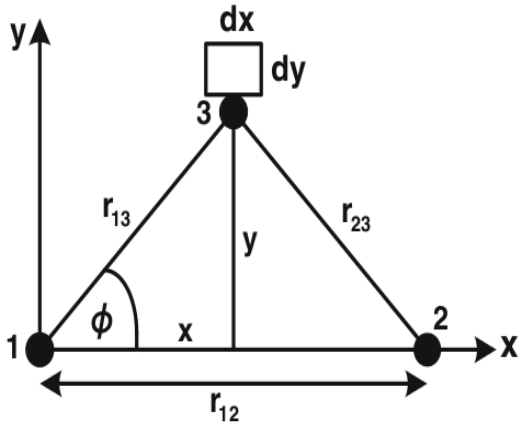

Figure A.1: Bipolar coordinates for three particle cluster

Appendix B

Value of M_k and q_N

From the equation (3.7) we can calculate M_1, M_2 and M_3,

$$M_1 = M_0 + \beta_1 \rho M_0. \tag{B.1}$$

$$M_2 = M_1 + \beta_1 \rho [M_1 - \frac{1}{N} M_0] + \frac{2\beta_2 \rho^2}{N} M_0. \tag{B.2}$$

$$M_3 = M_2 + \beta_1 \rho [M_2 - \frac{2}{N} M_1] + \frac{4\beta_2 \rho^2}{N} [M_1 - \frac{1}{N} M_0] + \frac{6\beta_3 \rho^3}{N^2} M_0.$$

where $M_0 = 1$ and M_3 is calculated approximatelly, because we are not considering β_3. So neglecting the term containing β_3, we get

$$M_3 \approx M_2 + \beta_1 \rho [M_2 - \frac{2}{N} M_1] + \frac{4\beta_2 \rho^2}{N} [M_1 - \frac{1}{N} M_0]. \tag{B.3}$$

The values of q_N is calculated using equation (3.6) as,

$$q_1 = M_1 - \frac{\beta_1 \rho}{N} M_0. \tag{B.4}$$

$$q_2 = M_2 - \frac{2\beta_1 \rho}{N} M_1 - \frac{4\beta_2 \rho^2}{N^2} M_0. \tag{B.5}$$

$$q_3 = M_3 - \frac{3\beta_1 \rho}{N} M_2 - \frac{12\beta_2 \rho^2}{N^2} M_1 - \frac{18\beta_3 \rho^3}{N^3} M_0. \tag{B.6}$$

In the above equation the term containing β_3 can be neglected so that the equation becomes

$$q_3 = M_3 - \frac{3\beta_1 \rho}{N} M_2 - \frac{12\beta_2 \rho^2}{N^2} M_1. \tag{B.7}$$